

**Last Revision  
June 30, 2023**

**ICE, CLOUD, and Land Elevation Satellite-2  
(ICESat-2) Project**

**Algorithm Theoretical Basis Document  
(ATBD)**

**for**

**Land-Ice Along-Track Products Part 2:  
Slope-Corrected Land Ice Height Time  
Series**

**Prepared By: Benjamin Smith, Suzanne Dickinson,  
Kaitlin Harbeck, Tom Neumann, David Hancock, Jeffrey Lee,  
Benjamin Jelley**

**This document may be cited as:**

Smith, B., S. Dickinson, K. Harbeck, T. Neumann, D. Hancock, J. Lee and B. Jelley (2023). *Ice, Cloud, and Land Elevation Satellite-2 (ICESat-2) Project Algorithm Theoretical Basis Document (ATBD) for Land-Ice Along-Track Products Part 2: Slope-Corrected Land Ice Height Time Series (ATL11)*, Version 6. ICESat-2 Project, DOI: 10.5067/ZQB1BP2DSTGM



**Goddard Space Flight Center  
Greenbelt, Maryland**

**National Aeronautics and  
Space Administration**

31

**Abstract**

32

33

**CM Foreword**

34 This document is an Ice, Cloud, and Land Elevation Satellite-2 (ICESat-2) Project Science  
35 Office controlled document. Changes to this document require prior approval of the Science  
36 Development Team ATBD Lead or designee. Proposed changes shall be submitted in the  
37 ICESat-II Management Information System (MIS) via a Signature Controlled Request (SCoRe),  
38 along with supportive material justifying the proposed change.

39 In this document, a requirement is identified by “shall,” a good practice by “should,” permission  
40 by “may” or “can,” expectation by “will,” and descriptive material by “is.”

41 Questions or comments concerning this document should be addressed to:

42 ICESat-2 Project Science Office

43 Mail Stop 615

44 Goddard Space Flight Center

45 Greenbelt, Maryland 20771

46

47

**Preface**

48

49 This document is the Algorithm Theoretical Basis Document for the TBD processing to be  
50 implemented at the ICESat-2 Science Investigator-led Processing System (SIPS). The SIPS  
51 supports the ATLAS (Advance Topographic Laser Altimeter System) instrument on the ICESat-  
52 2 Spacecraft and encompasses the ATLAS Science Algorithm Software (ASAS) and the  
53 Scheduling and Data Management System (SDMS). The science algorithm software will produce  
54 Level 0 through Level 4 standard data products as well as the associated product quality  
55 assessments and metadata information.

56 The ICESat-2 Science Development Team, in support of the ICESat-2 Project Science Office  
57 (PSO), assumes responsibility for this document and updates it, as required, as algorithms are  
58 refined or to meet the needs of the ICESat-2 SIPS. Reviews of this document are performed  
59 when appropriate and as needed updates to this document are made. Changes to this document  
60 will be made by complete revision.

61 Changes to this document require prior approval of the Change Authority listed on the signature  
62 page. Proposed changes shall be submitted to the ICESat-2 PSO, along with supportive material  
63 justifying the proposed change.

64 Questions or comments concerning this document should be addressed to:

65 Thorsten Markus, ICESat-2 Project Scientist

66 Mail Stop 615

67 Goddard Space Flight Center

68 Greenbelt, Maryland 20771

69

70

**Review/Approval Page**

***Prepared by:***

Benjamin Smith  
Principal Researcher  
University of Washington  
Applied Physics Lab Polar Science Center  
1013 NE 40th Street  
Box 355640  
Seattle, WA 98105

***Reviewed by:***

*Shane Grigsby*  
*Postdoctoral Scholar*  
*Colorado School of Mines*  
*Department of Geophysics*

*Ellen Enderlin*  
*Assistant Professor*  
*Department of Geosciences*  
*Boise State University*

***Approved by:***

*Tom Neumann*  
*Project Scientist*  
*Code 615*

71

72

73

\*\*\* Signatures are available on-line at: <https://icesatiimis.gsfc.nasa.gov> \*\*\*

**Change History Log**

Revision Level	Description of Change	SCoRe No.	Date Approved
1.0	Initial Release		
1.1	Changes for release 002. Calculate all crossovers (including near 88 S), determine the center of the y_atc search from the median of unique pair center locations.		
1.2	Changes for release 003. Add geoid and dem parameters.		
1.3	Improved the description of the polynomial coefficient writing process		
1.4	Changes for release 005: Updated geoid description, changed product name		
1.5	Changes for release 006: Added Antarctic geolocation correction, removed all references to the slope_change_rate calculation Limit y degree to 1 unless there is an adequate cross-track distribution of pair y values.		

75

**List of TBDs/TBRs**

Item No.	Location	Summary	Ind./Org.	Due Date

76

77	<b>Table of Contents</b>		
78	Abstract .....		ii
79	CM Foreword .....		iii
80	Preface .....		iv
81	Review/Approval Page .....		v
82	Change History Log .....		vi
83	List of TBDs/TBRs .....		vii
84	Table of Contents .....		viii
85	List of Figures .....		x
86	List of Tables .....		xi
87	1.0 INTRODUCTION .....		1
88	2.0 BACKGROUND INFORMATION and OVERVIEW .....		2
89	2.1 Background .....		2
90	2.2 Elevation-correction Coordinate Systems .....		3
91	2.3 Terminology: .....		3
92	2.4 Repeat and non-repeat cycles in the ICESat-2 mission .....		5
93	2.5 Physical Basis of Measurements / Summary of Processing .....		5
94	2.5.1 Choices of product dimensions .....		6
95	2.6 Product coverage .....		6
96	3.0 ALGORITHM THEORY: Derivation of Land Ice H (t)/ATL11 (L3B) .....		8
97	3.1 Input data editing .....		10
98	3.1.1 Input data editing using ATL06 parameters .....		11
99	3.1.2 Input data editing by slope .....		12
100	3.1.3 Spatial data editing .....		13
101	3.2 Reference-Surface Shape Correction .....		13
102	3.2.1 Reference-surface shape inversion .....		14
103	3.2.2 Misfit analysis and iterative editing .....		15
104	3.3 Reference-shape Correction Error Estimates .....		15
105	3.4 Calculating corrected height values for repeats with no selected pairs .....		16
106	3.5 Calculating systematic error estimates .....		16
107	3.6 Calculating shape-corrected heights for crossing-track data .....		17
108	3.7 Calculating parameter averages .....		18



*ICESat-2 Algorithm Theoretical Basis Document for Land Ice H(t) (ATL11)*

*Release 006*

109	3.8	Output data editing .....	18
110	3.9	Antarctic geolocation biases .....	18
111	3.9.1	Estimating Antarctic geolocation biases .....	18
112	3.9.2	Correcting for Antarctic geolocation biases. ....	21
113	4.0	LAND ICE PRODUCTS: Land Ice H (t)(ATL 11/L3B) .....	23
114	4.1	File naming convention .....	23
115	4.2	/ptx group .....	23
116	4.3	/ptx/ref_surf group .....	24
117	4.4	/ptx/cycle_stats group .....	26
118	4.5	/ptx/crossing_track_data group .....	28
119	5.0	ALGORITHM IMPLEMENTATION .....	31
120	5.1.1	Select ATL06 data for the current reference point.....	32
121	5.1.2	Select pairs for the reference-surface calculation .....	32
122	5.1.3	Adjust the reference-point y location to include the maximum number of	
123	cycles	35	
124	5.1.4	Calculate the reference surface and corrected heights for selected pairs	35
125	5.1.5	Calculate corrected heights for cycles with no selected pairs. ....	38
126	5.1.6	Calculate corrected heights for crossover data points.....	39
127	5.1.7	Provide error-averaged values for selected ATL06 parameters.....	40
128	5.1.8	Provide miscellaneous ATL06 parameters .....	41
129	5.1.9	Characterize the reference surface .....	42
130	6.0	Appendix A: Glossary .....	44
131	7.0	Browse products.....	50
132		Glossary/Acronyms.....	56
133		References .....	57
134			

135 **List of Figures**

136		
137	<u>Figure</u>	<u>Page</u>
138	Figure 2-1. ICESat-2 repeat-track schematic.....	3
139	Figure 2-2. ATL06 data for an ATL11 reference point.....	4
140	Figure 2-3. Potential ATL11 coverage.....	6
141	Figure 3-1. ATL11 fitting schematic.....	9
142	Figure 3-2. Data selection.....	11
143	Figure 5-1 Flow Chart for ATL11 Surface-shape Corrections.....	31
144	Figure 6-1. Spots and tracks, forward flight.....	47
145	Figure 6-2. Spots and tracks, backward flight.....	48
146	Figure 6-3. Granule regions.....	49
147		

148

**List of Tables**

149

150 Table Page

151 Table 3-1 Parameter Filters to determine the validity of segments for ATL11 estimates ..... 10

152 Table 4-1 Parameters in the */ptx/* group ..... 24

153 Table 4-2 Parameters in the */ptx/ref\_surf* group ..... 25

154 Table 4-3 Parameters in the */ptx/cycle\_stats* group ..... 27

155 Table 4-4 Parameters in the */ptx/crossing\_track\_data* group ..... 30

156

157 **1.0 INTRODUCTION**

158 This document describes the theoretical basis and implementation of the level-3b land-ice  
159 processing algorithm for ATL11, which provides time series of surface heights. The higher-level  
160 products, providing gridded height, and gridded height change will be described in supplements  
161 to this document available in early 2020.

162 ATL11 is based on the ICESat-2 ATL06 Land-ice Height product, which is described  
163 elsewhere (Smith and others, 2019a, Smith and others, 2019b). ATL06 provides height estimates  
164 for 40-meter overlapping surface segments, whose centers are spaced 20 meters along each of  
165 ICESat-2's RPTs (reference pair tracks), but displaced horizontally both relative to the RPT and  
166 relative to one another because of small (a few tens of meters or less) imprecisions in the  
167 satellite's control of the measurement locations on the ground. ATL11 provides heights  
168 corrected for these offsets between the reference tracks and the location of the ATLAS  
169 measurements. It is intended as an input for high-level products, ATL15 and ATL16, which  
170 will provide gridded estimates of ice-sheet height and height change, but also may be used alone,  
171 as a spatially-organized product that allows easy access to height-change information derived  
172 from ICESat-2.

173 ATL11 employs a technique which builds upon those previously used to measure short-term  
174 elevation changes using ICESat repeat-track data. Where surface slopes are small and the  
175 geophysical signals are large compared to background processes (i.e., ice plains and ice shelves),  
176 some studies have subtracted the mean from a collection of height measurements from the same  
177 repeat track to leave the rapidly-changing components associated with subglacial water motion  
178 (Fricker and others, 2007) or tidal flexure (Brunt and others, 2011). In regions where off-track  
179 surface slopes are not negligible, height changes can be recovered if the mean height and an  
180 estimate of the surface slope (Smith and others, 2009) are subtracted from the data, although in  
181 these regions the degree to which the surface slope estimate and the elevation-change pattern are  
182 independent is challenging to quantify.

183 ICESat-2's ATL06 product provides both surface height and surface-slope information each time  
184 it overflies its reference tracks. The resulting data are similar to that from the scanning laser  
185 altimeters that have been deployed on aircraft in Greenland and Antarctica for two decades  
186 (cite), making algorithms originally developed for these instruments appropriate for use in  
187 interpreting ATLAS data. One example is the SERAC (Surface Elevation Reconstruction and  
188 Change Detection) algorithm (Schenk & Csatho, 2012) provides an integrated framework for the  
189 derivation of elevation change from altimetry data. In SERAC, polynomial surfaces are fit to  
190 collections of altimetry data in small (< 1 km) patches, and these surfaces are used to correct the  
191 data for sub-kilometer surface topography. The residuals to the surface then give the pattern of  
192 elevation change, and polynomial fits to the residuals as a function of time give the long-term  
193 pattern of elevation change. The ATL11 algorithm is similar to SERAC, except that (1)  
194 polynomial fit correction is formulated somewhat differently, so that the ATL11 correction gives  
195 the surface height at the fit center, not the height residual, and (2) ATL11 does not include a  
196 polynomial fit with respect to time.

197

## 198 2.0 BACKGROUND INFORMATION AND OVERVIEW

199 This section provides a conceptual description of ICESat-2's ice-sheet height measurements and  
200 gives a brief description of the derived products.

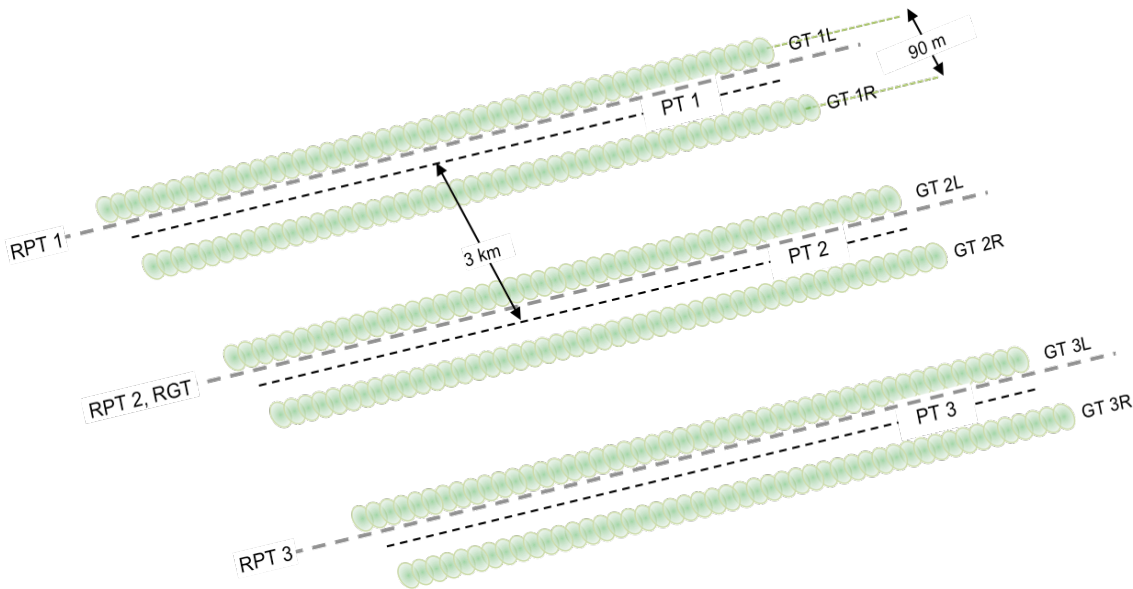
### 201 2.1 Background

202 The primary goal of the ICESat-2 mission is to estimate mass-balance rates for the Earth's ice  
203 sheets. An important step in this process is the calculation of height change at specific locations  
204 on the ice sheets. In an ideal world, a satellite altimeter would exactly measure the same point  
205 on the earth on each cycle of its orbit. However, there are limitations in a spacecraft's ability to  
206 exactly repeat the same orbit and to point to the same location. These capabilities are greatly  
207 improving with technological advances but still have limits that need to be accounted for when  
208 estimating precise elevation changes from satellite altimetry data. The first ICESat mission  
209 allowed estimates of longer-term elevation rates using along-track differencing, because  
210 ICESat's relatively precise (50-150-m) pointing accuracy, precise (4-15 m) geolocation  
211 accuracy, and small (35-70-m) footprints allowed it to resolve small-scale ice-sheet topography.  
212 However, because ICESat had a single-beam instrument, its repeat-track measurements were  
213 reliable only for measuring the mean rate of elevation change, because shorter-term height  
214 differences could be influenced by the horizontal dispersion of tracks on a sloping surface.  
215 ICESat-2 makes repeat measurements over a set of 1387 reference ground tracks (RGTs),  
216 completing a *cycle* over all of these tracks every 91 days. ICESat-2's ATLAS instrument  
217 employs a split-beam design, where each laser pulse is divided six separate beams. The beams  
218 are organized into three *beam pairs*, with each separated from its neighbors by 3.3 km (**Figure**  
219 **2-1**), each pair following a reference pair track (RPT) that is parallel to the RGT. The beams  
220 within each pair separated by 90 m, which means that each cycle's measurement over an RPT  
221 can determine the surface slope independently, and a height difference can be derived from  
222 any two measurements of an RPT. The 90-m spacing between the laser beams in each pair  
223 is equal to twice the required RMS accuracy with which ICESat-2 can be pointed at its RPTs,  
224 which means that for most, but not all, repeat measurements of a given RPT, the pairs of  
225 beams will overlap one another. To obtain a record of elevation change from the collection  
226 of paired measurements on each RPT, some correction is still necessary to account for the  
227 effects of small-scale surface topography around the RPT in the ATL06 surface heights that  
228 appear as a result of this non-exact pointing. ATL11 uses a polynomial fit to the ATL06  
229 measurements to correct for small-scale topography effects on surface heights that result  
230 from this non-exact pointing.

231 The accuracy of ICESat-2 measurements depends on the thickness of clouds between the  
232 satellite and the surface, on the reflectance, slope, and roughness of the surface, and on  
233 background noise rate which, in turn, depends on the intensity of solar illumination of the  
234 surface and the surface reflectance. It also varies from laser beam to beam, because in each  
235 of ICESat-2's beam pairs one beam (the "strong beam") has approximately four times the  
236 signal strength of the other (the "weak beam"). Parameters on the ATL06 product allow  
237 estimation of errors in each measurement, and allow filtering of most measurements with  
238 large errors due to misidentification of clouds or noise as surface returns (blunders), but to  
239 enable higher precision surface change estimates, ATL11 implements further self-  
240 consistency checks that further reduce the effects of errors and blunders.

241

Figure 2-1. ICESat-2 repeat-track schematic



Schematic drawing showing the pattern made by ATLAS's 6-beam configuration on the ground, for a track running from lower left to upper right. The 6 beams are grouped into 3 beam pairs with a separation between beams within a pair of 90m and a separation between beam pairs of 3.3 km. The RPTs (Reference Pair Tracks, heavily dashed lines in gray) are defined in advance of launch; the central RPT follows the RGT (Reference Ground Track, matching the nadir track of the predicted orbit). The Ground Tracks are the tracks actually measured by ATLAS (GT1L, GT1R, etc., shown by green footprints). Measured Pair Tracks (PTs, smaller dashed lines in black) are defined by the centers of the pairs of GTs, and deviate slightly from the RPTs because of inaccuracies in repeat-track pointing. The separation of GTs in each pair in this figure is greatly exaggerated relative to the separation of the PTs.

242 **2.2 Elevation-correction Coordinate Systems**

243 We perform ATL11 calculations using the along-track coordinate system described in the  
 244 ATL06 ATBD (Smith and others, 2019b, Smith and others, 2019a). The along-track coordinate  
 245 is measured parallel to the RGT, starting at each RGT's origin at the equator. The across-track  
 246 coordinate is measured to the left of the RGT, so that the two horizontal basis vectors and the  
 247 local vertical vector form a right-handed coordinate system.

248 **2.3 Terminology:**

249 Some of the terms that we will use in describing the ATL11 fitting process and the data  
 250 contributing are:

251 *RPT*: Reference pair track

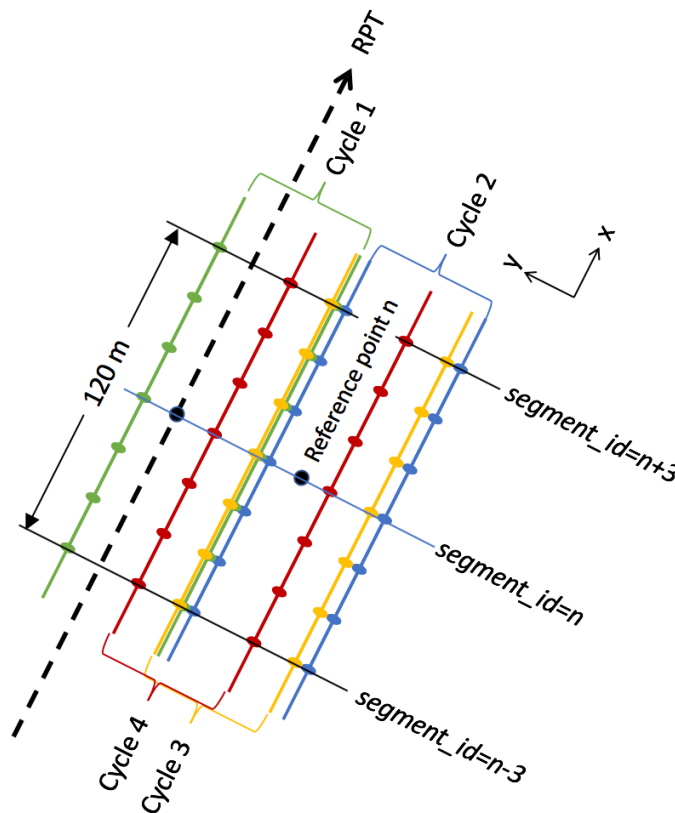
252 *Cycle*: ICESat-2 has 1387 distinct reference ground tracks, which its orbit covers every 91 days.

253 One repeat measurement of these reference ground tracks constitutes a cycle.

254 *ATL06 segment*: A 40-meter segment fit to a collection of ATL03 photon-event data, as  
 255 described in the ATL06 ATBD  
 256 *ATL06 pair*: Two ATL06 segments from the same cycle with the same *segment\_id*. By  
 257 construction, both segments in the ATL06 pair have the same along-track coordinate, and are  
 258 separated by the beam-to-beam spacing (approximately 90 m) in the across-track direction  
 259 *ATL11 RPT point*: The expected location of each ATL11 point on the RPT, equivalent to the  
 260 beginning of every third geosegment on the RPT, or the center of every third ATL06 segment.  
 261 *ATL11 reference point*: an *ATL11 RPT point* shifted in the across-track direction to better match  
 262 the geometry of the available ATL06 data.  
 263 *ATL11 fit*: The data and parameters associated with a single ATL11 reference point. This  
 264 includes corrected heights from all available cycles  
 265

266 ATL11 calculates elevations and elevation differences based on collections of segments from the  
 267 same beam pair but from different cycles. ATL11 is posted every 60 m, which corresponds to  
 268 every third ATL06 *segment\_id*, and includes ATL06 segments spanning three segments before  
 269 and after the central segment, so that the ATL11 uses data that span 120 m in the along-track  
 270 direction. ATL11 data are centered on *reference points*, which has the same along-track  
 271 coordinate as its central ATL06 segment, but is displaced in the across-track direction to better  
 272 match the locations of the ATL06 measurements from all of the cycles present (see section  
 273 3.1.3).

Figure 2-2. ATL06 data for an ATL11 reference point



Schematic of ATL06 data for an ATL11 reference point centered on segment n, based on data from four cycles. The segment centers span 120 m in the along-track data, and the cycles are randomly displaced from

the RPT in the across-track direction. The reference point has an along-track location that matches that of segment n, and an across-track position chosen to match the displacements of the cycles.

274

#### 275 **2.4 Repeat and non-repeat cycles in the ICESat-2 mission**

276 In the early part of the ICESat-2 mission, an error in the configuration of the start trackers  
277 prevented the instrument from pointing precisely at the RGTs. As a result, all data from cycles 1  
278 and 2 were measured between one and two kilometers away from the RGTs, with offsets that  
279 varied in time and as a function of latitude. The measurements from cycles 1 and 2 still give  
280 high-precision measurements of surface height, but repeat-track measurements from ICESat-2  
281 begin during cycle 3, in April of 2019. ATL11 files will be generated for ATL06 granules from  
282 cycles 1 and 2, but these will contain only one cycle of data, plus crossovers, because the  
283 measurements from these cycles (which are displaced from the RPTs by several kilometers) will  
284 not be repeated. We expect the measurements from cycles 1 and 2 to be useful as a reduced-  
285 resolution (compared to ATL06) mapping of the ice sheet, which may prove useful in DEM  
286 generation and in comparisons with other altimetry missions. For cycles 3 and after, each  
287 ATL11 granule will contain all available cycles for each RGT (i.e. from cycle 3 onwards), and  
288 will contain crossovers between the repeat cycles and cycles 1 and 2.

289 Outside the polar regions, ICESat-2 is pointed to minimize gaps between repeat measurements,  
290 and so does not make repeat measurements over its ground tracks. ATL11 is only calculated  
291 within the repeat-pointing mask (see Figure ???), which covers areas poleward of 60°N and  
292 60°S.  
293

#### 294 **2.5 Physical Basis of Measurements / Summary of Processing**

295 Surface slopes on the Antarctic and Greenland ice sheets are generally small, with magnitudes  
296 less than two degrees over 99% of Antarctica's area. Smaller-scale (0.5-3 km) undulations,  
297 generated by ice flow over hilly or mountainous terrain may have amplitudes of up to a few  
298 degrees. Although we expect that the surface height will change over time, slopes and locations  
299 of these smaller-scale undulation are likely controlled by underlying topography and should  
300 remain essentially constant over periods of time comparable with the expected 3-7 duration of  
301 the ICESat-2 mission. This allows us to use estimates of ice-sheet surface shape derived from  
302 data spanning the full mission to correct for small (<130-m) differences in measurement  
303 locations between repeat measurements of the same RPT, to produce records of height change  
304 for specific locations. Further, we can use the surface slope estimates in ATL06 to determine  
305 whether different sets of measurements for the same fit center are self-consistent: We can assume  
306 that if an ATL06 segment shows a slope significantly different from others measured near the  
307 same reference point it likely is in error. The combination of parameters from ATL06 and these  
308 self-consistency checks allows us to generate time series based on the highest-quality  
309 measurements for each reference point, and our reference surface calculation lets us correct for  
310 small-scale topography and to estimate error magnitudes in the corrected data.

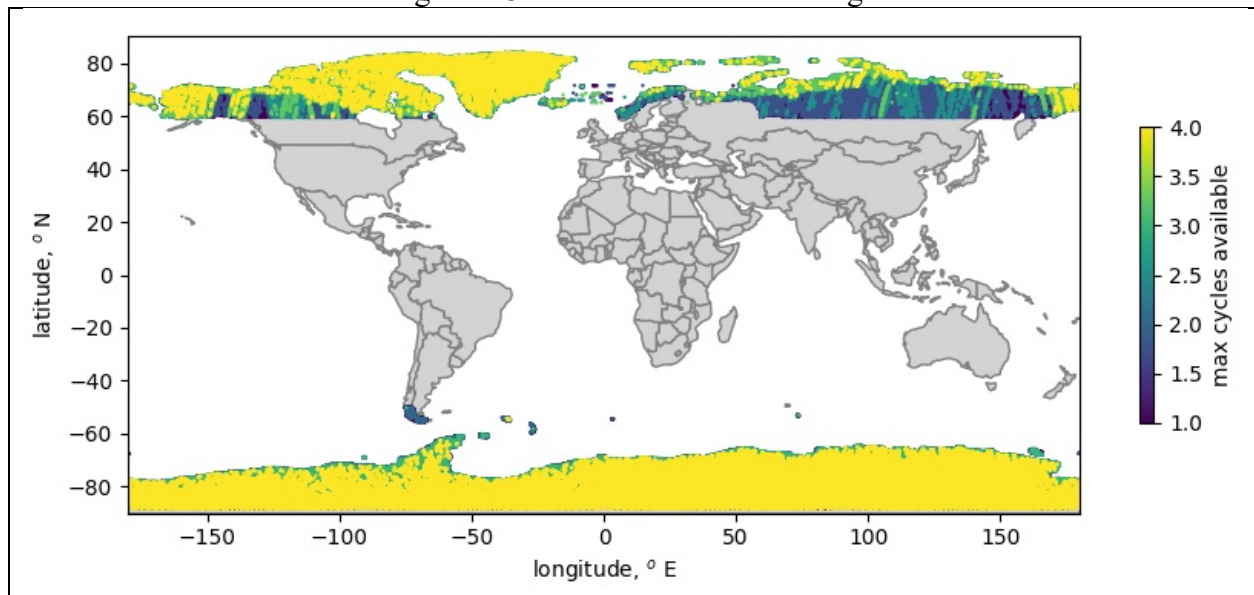


311 **2.5.1 Choices of product dimensions**

312 We have chosen a set of dimensions for the ATL11 fitting process with the goal of creating a  
 313 product that is conveniently sized for analysis of elevation changes, while still capturing the  
 314 details of elevation change in outlet glaciers. The assumption that ice-sheet surface can be  
 315 approximated by a low-degree polynomial becomes untenable as data from larger and larger  
 316 areas are included in the calculation; therefore we use data from the smallest feasible area to  
 317 define our reference surface, while still including enough data to reduce the sampling error in the  
 318 data and to allow for the possibility that at least one or two will encounter a flat surface, which  
 319 greatly improves the chances that each cycle will be able to measure surface comparable to one  
 320 another. Each ATL11 point uses data from an area up to 120 m in the along-track direction by  
 321 up to 130 m in the across-track direction. We have chosen the cross-track search distance  
 322 ( $L_{search\_XT}$ ) to be 65 m, approximately equal to half the beam spacing, plus three times the  
 323 observed 6.5 m standard deviation of the across-track pointing accuracy for cycles 3 and 4 in  
 324 Antarctica. We chose the across-track search distance ( $L_{search\_AT}$ ) to be 60 m, approximately  
 325 equal to  $L_{search\_XT}$ , so that the full  $L_{search\_AT}$  search window spans three ATL06 segments before  
 326 and after the central segment for each reference point. The resulting along-track resolution is  
 327 around one third that of ATL06, but still allows 6-7 distinct elevation-change samples across a  
 328 small (1-km) outlet glacier.

329 **2.6 Product coverage**

Figure 2-3. Potential ATL11 coverage



Maximum number of valid repeat measurements from an ATL11 file for each 10-km segment of pair track 2. Yellower colors indicate areas where ICESat-2 has systematically pointed at the RGTs.

330 Over the vegetated parts of the Earth, ICESat-2 makes spatially dense measurements, measuring  
 331 tracks parallel to the reference tracks in a strategy that will eventually measure global vegetation  
 332 with a track-to-track spacing better than 1 km. Because ATL11 relies upon repeat measurements  
 333 over reference tracks to allow the calculation of its reference surfaces, ATL11 is generated for  
 334 ICESat-2 subregions 3-5 and 10-12 (global coverage, north and south of 60 degrees). Repeat

335 measurements are limited to Antarctica, Greenland, and the High Arctic islands (Figure 2-3),  
336 although in other areas the fill-in strategy developed for vegetation measurements allows some  
337 repeat measurements. In regions where ICESat-2 was not pointed to the repeat track, most  
338 ATL11 reference points will provide one measurement close to the RPT. Crossover data are  
339 available for many of these points, though their distribution in time is not regular. A future  
340 update to the product may provide crossover measurements for lower-latitude areas, but the  
341 current product format is not designed to allow this.

342 **3.0 ALGORITHM THEORY: DERIVATION OF LAND ICE H (T)/ATL11 (L3B)**

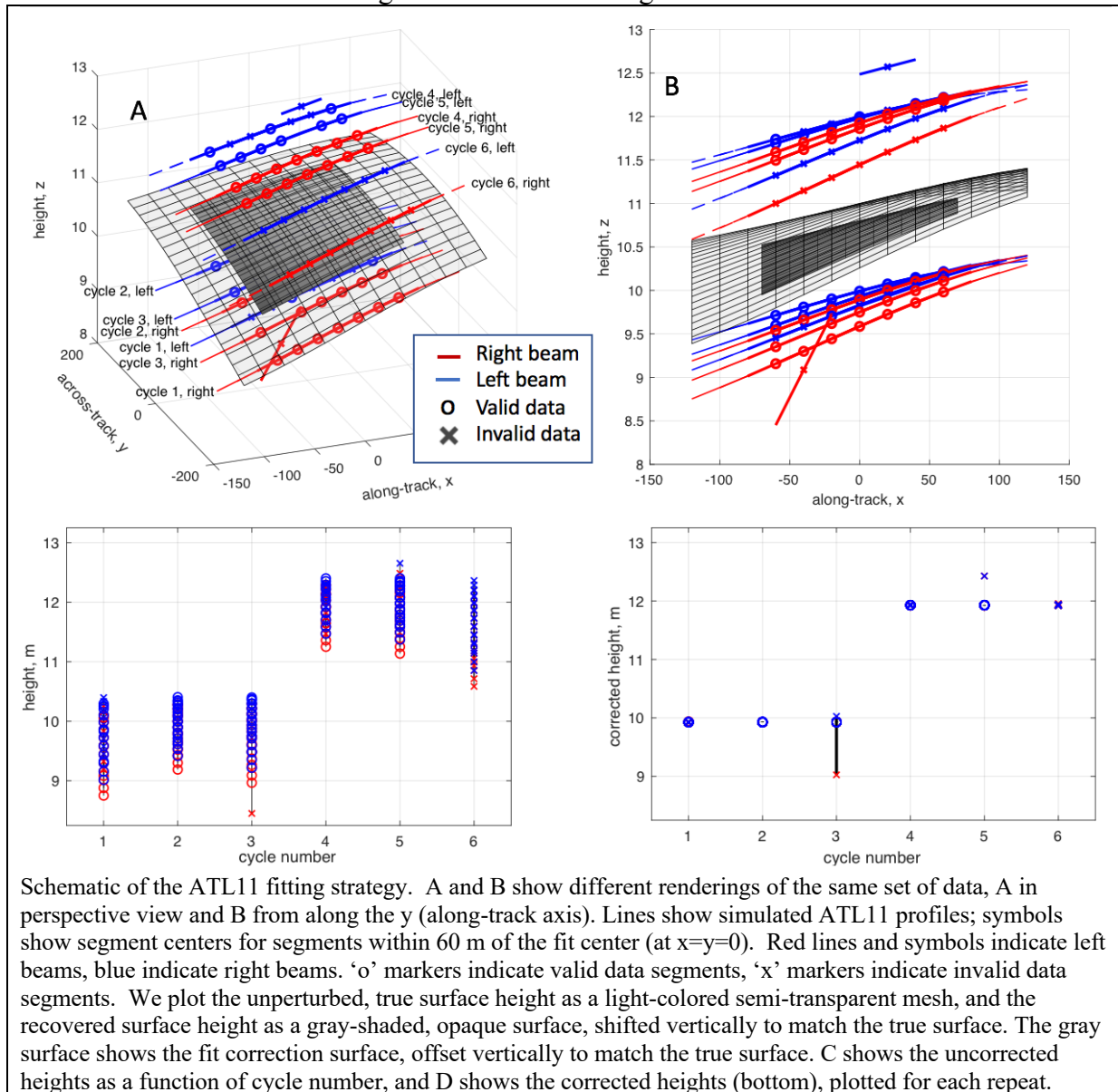
343 In this section, we describe in detail the algorithms used in calculating the ATL11 land-ice  
344 parameters. This product is intended to provide time series of surface heights for land-ice and  
345 ice-shelf locations where ICESat-2 operates in repeat-track mode (*i.e.* for polar ice), along with  
346 parameters useful in determining whether each height estimate is valid or a result of a variety of  
347 potential errors (see ATL06 ATBD, section 1).

348 ATL11 height estimates are generated by correcting ATL06 height measurements for the  
349 combined effects of short-scale (40-120-m) surface topography around the fit centers and small  
350 (up to 130-m) horizontal offsets between repeat measurements. We fit a polynomial reference  
351 surface to height measurements from different cycles as a function of horizontal coordinates  
352 around the fit centers, and use this polynomial surface to correct the height measurements to the  
353 fit center. The resulting values reflect the time history of surface heights at the reference points,  
354 with minimal contributions from small-scale local topography.

355 In this algorithm, for a set of reference points spaced every 60 meters along each RPT (centered  
356 on every third segment center), we consider all ATL06 segments with centers within 60 m along-  
357 track and 65 m across-track of the reference point, so that each ATL11 fit contains as many as  
358 seven distinct along-track segments from each laser beam and cycle. We select a subset of these  
359 segments with consistent ATL06 slope estimates and small error estimates, and use these  
360 segments to define a time-variable surface height and a polynomial surface-shape model. We  
361 then use the surface-shape model to calculate corrected heights for the segments from cycles not  
362 included in the initial subset. We propagate errors for each of these steps to give formal errors  
363 estimates that take into account the sampling error from ATL06, and propagate the geolocation  
364 errors with the slope of the surface-shape model to give an estimate of systematic errors in the  
365 height estimates.  
366

367

Figure 3-1. ATL11 fitting schematic



368

369

370

371

372

373

374

375

376

377

Figure 3-1 shows a schematic diagram of the fitting process. In this example, we show simulated ATL06 height measurements for six 91-day orbital cycles over a smooth ice-sheet surface (transparent grid). Between cycles 3 and 4, the surface height has risen by 2 m. Two of the segments contain errors: The weak beam for one segment from repeat 3 is displaced downward and has an abnormal apparent slope in the  $x$  direction, and one segment from repeat 5 is displaced upwards, so that its pair has an abnormal apparent slope in the  $y$  direction. Segments falling within the across and along-track windows of the reference point (at  $x=y=0$  in this plot) are selected, and fit with a polynomial reference surface (shown in gray). When plotted as a function of cycle number (panel C), the measured heights show considerable scatter but when

378 corrected to the reference surface (panel D), each cycle shows a consistent height, and the  
 379 segments with errors are clearly distinct from the accurate measurements.

380 **3.1 Input data editing**

381 Each ATL06 measurement includes location estimates, along- and across-track slope estimates,  
 382 and PE (Photon-Event)-height misfit estimates. To calculate the reference surface using the most  
 383 reliable subset of available data, we perform tests on the surface-slope estimates and error  
 384 statistics from each ATL06-pair to select a self-consistent set of data. These tests determine  
 385 whether each pair of measurements is *valid* and can be used in the reference-shape calculation or  
 386 is *invalid*. Segments from invalid pairs may be used in elevation-change calculations, but not in  
 387 the reference-shape calculation.

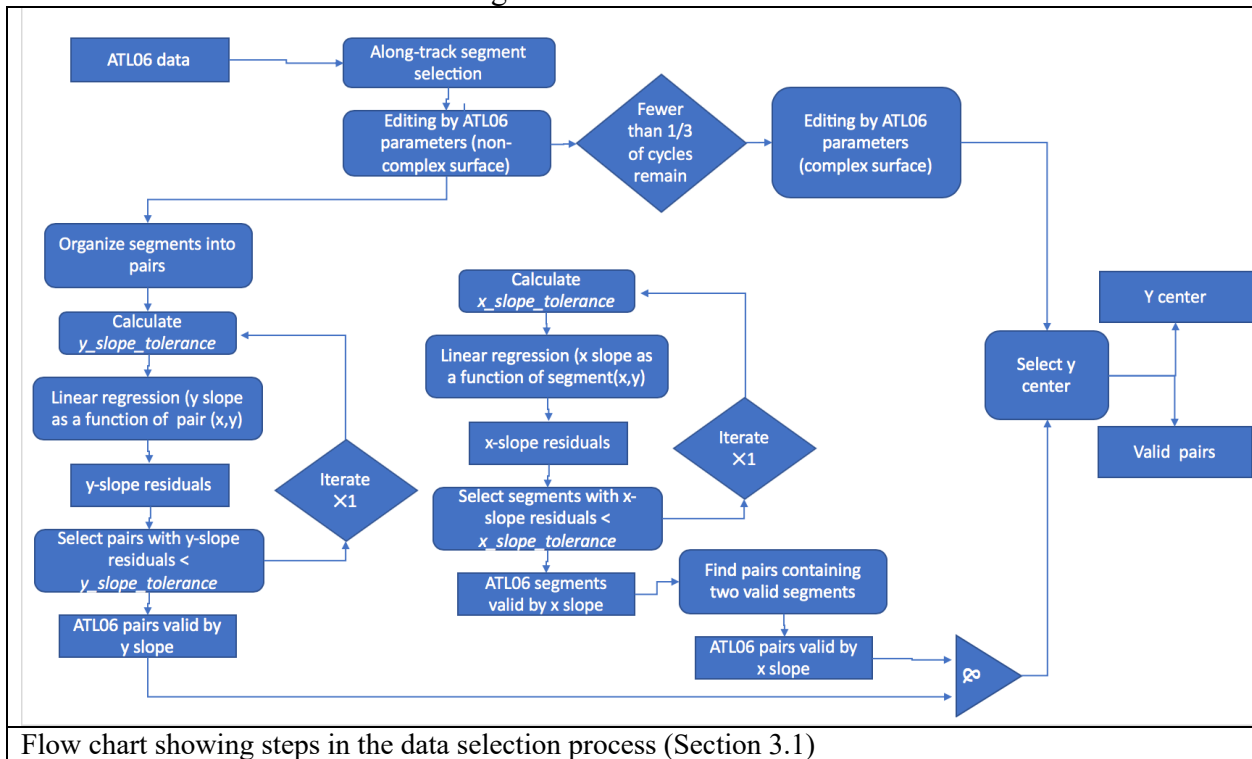
388 A complete flow chart of the data-selection process is shown in Figure 3-2, and the parameters  
 389 used to make these selections and their values are listed in Table 3-1.

390

391 **Table 3-1 Parameter Filters to determine the validity of segments for ATL11 estimates**

complex_surface_flag	Segment parameter	Filter strategy	Section
0	<i>ATL06_quality_summary</i>	<i>ATL06_quality_summary</i> =0 (indicates high-quality segments)	3.1.1
1	<i>SNR_significance</i>	<i>SNR_significance</i> < 0.02 (indicates low probability of surface-detection blunders)	3.1.1
0 or 1	Along-track differences	Minimum height difference between the endpoints of a segment and the middles of its neighbors must be < 2 m (for smooth surfaces) or < 10 m (for complex surfaces)	3.1.1
0 or 1	<i>h_li_sigma</i>	<i>h_li_sigma</i> < max(0.05, 3*median( <i>h_li_sigma</i> ))	3.1.1
0 or 1	Along-track slope	<i>r_slope_x</i>   < 3 <i>slope_tolerance_x</i>	3.1.2
0 or 1	Across-track slope	<i>r_slope_y</i>   < 3 <i>slope_tolerance_y</i>	3.1.2
0 or 1	Segment location	<i>x_atc-x0</i>   < <i>L_search_XT</i>   <i>y_atc-y0</i>   < <i>L_search_AT</i>	3.1.3

Figure 3-2. Data selection



392

### 393 3.1.1 Input data editing using ATL06 parameters

394 For each reference point, we collect all ATL06 data from all available repeat cycles that have  
 395 *segment\_id* values within  $\pm 3$  of the reference point (inclusive) and that are on the same *rgt* and  
 396 pair track as the reference point. The *segment\_id* criterion ensures that the segment centers are  
 397 within  $\pm 60$  m of the reference point in the along-track direction. We next check that the ATL06  
 398 data are close to the pre-defined reference track, by rejecting all ATL06 segments that are more  
 399 than 500 m away from the nominal pair across-track coordinates (-3200, 0, and 3200 meters for  
 400 right, center, and left pairs, respectively). This removes data that were intentionally or  
 401 accidentally collected with ATLAS pointed off nadir (i.e. for calibration scan maneuvers).

402 ATL06 contains some segments with signal-finding blunders (Smith et al., 2019). To avoid  
 403 having these erroneous segments contaminate ATL11, we filter using one of two sets of tests,  
 404 depending on surface roughness. We identify high-quality ATL06 segments, using parameters  
 405 that depend on whether the surface is identified as smooth or rough, as follows:

406 1) For smooth ice-sheet surfaces, we use the ATL06 *ATL06\_quality\_summary* parameter,  
 407 combined with a measure of along-track elevation consistency, *at\_min\_dh*, that is calculated as  
 408 part of ATL11. *ATL06\_quality\_summary* is based on the spread of the residuals for each  
 409 segment, the along-track surface slope, the estimated error, and the signal strength. Zero values  
 410 indicate that no error has been found. We define the along-track consistency parameter  
 411 *at\_min\_dh* as the minimum absolute difference between the heights of the endpoints of each  
 412 segment and the center heights of the previous and subsequent segments. Its value will be small  
 413 if a segment's height and slope are consistent with at least one of its neighbors. For smooth

414 surfaces, we require that the *at\_min\_dh* values be less than 2 m. Over smooth ice-sheet surfaces,  
 415 the 2-m threshold eliminates most blunders without eliminating a substantial number of high-  
 416 quality data points.

417 2) For rough, crevassed surfaces, the smooth-ice strategy may not identify a sufficient number of  
 418 pairs for ATL11 processing to continue. If fewer than one third of the original cycles remain  
 419 after the smooth-surface criteria are applied, we relax our criteria, using the signal-to-noise ratio  
 420 (based on the ATL06 *segment\_stats/snr\_significance* parameter) to select the pairs to include in  
 421 the fit, and require that the *at\_min\_dh* values be less than 10 m. If we relax the criteria in this  
 422 way, we mark the reference point as having a complex surface using the  
 423 *ref\_surf/complex\_surface\_flag*, which limits the degree of the polynomial used in the reference  
 424 surface fitting to 0 or 1 in each direction.

425 For either smooth or rough surfaces, we perform an additional check using the magnitude of  
 426 *h\_li\_sigma* for each segment. If any segment's value is larger than three times the maximum of  
 427 0.05 m and the median *h\_li\_sigma* for the valid segments for the current reference point, it is  
 428 marked as invalid. The limiting 0.05 m value prevents this test from removing high-quality data  
 429 over smooth ice-sheet surfaces, where errors are usually small.

430 Each of these tests applies to values associated with ATL06 segments. When the tests are  
 431 complete, we check each ATL06 pair (*i.e.* two segments for the same along-track location from  
 432 the same cycle) and if either of its two segments has been marked as invalid, the entire pair is  
 433 marked as invalid.

### 434 3.1.2 Input data editing by slope

435 The segments selected in 3.1.1 may include some high-quality segments and some lower-quality  
 436 segments that were not successfully eliminated by the data-editing criteria. We expect that the  
 437 ATL06 slope fields (*dh\_fit\_dx*, and *dh\_fit\_dy*) for the higher-quality data should reflect the  
 438 shape of an ice-sheet surface with a spatially consistent surface slope around each reference  
 439 point, but that at least some of lower-quality data should have slope fields that outliers relative to  
 440 this consistent surface slope. In this step, we assume that the slope may vary linearly in *x* and *y*,  
 441 and so use residuals between the slope values and a regression of the slope values against *x* and *y*  
 442 to identify the data with inconsistent slope values. The data with large residuals are marked as  
 443 *invalid*.

444 Starting with valid pairs from 3.2.1, we first perform a linear regression between the *y* slopes of  
 445 the pairs and the pair-center *x* and *y* positions. The residuals to this regression define one  
 446 *y\_slope\_residual* for each pair. We compare these residuals against a *y\_slope\_tolerance*:

$$y\_slope\_tolerance = \max(0.01, 3 \text{ median } (dh\_fit\_dy\_sigma), 3 RDE \quad 1 \\ (y\_slope\_residuals))$$

447 Here RDE is the Robust Difference Estimator, equal to half the difference between the 16<sup>th</sup> and  
 448 84<sup>th</sup> percentiles of a distribution, and the minimum value of 0.01 ensures that this test does not  
 449 remove high-quality segments in regions where the residuals are very consistent. If any pairs  
 450 have a *y\_slope\_residual* greater than *y\_slope\_tolerance*, we remove them from the group of valid  
 451 pairs, then repeat the regression, recalculate *y\_slope\_tolerance*, and retest the remaining pairs.  
 452 We then return to the pairs marked as *valid* from 3.1.1, and perform a linear regression between  
 453 the *x* slopes of the segments within the pairs and the segment-center *x* and *y* positions. The  
 454 residuals to this regression define one *x\_slope\_residual* for each segment. We compare these

455 residuals against an  $x_{slope\_tolerance}$ , calculated in the same way as (1), except using segment  $x$   
 456 slopes and residuals instead of pair  $y$  slopes. As with the  $y$  regression, we repeat this procedure  
 457 once if any segments are eliminated in the first round.

458 After both the  $x$  and  $y$  regression procedures are complete, each pair of segments is marked as  
 459 *valid* if both of its  $x$  residuals are smaller than  $slope\_tolerance\_x$  and its  $y$  residual is smaller than  
 460  $slope\_tolerance\_y$ .

### 461 3.1.3 Spatial data editing

462 The data included in the reference-surface fit fall in a “window” defined by a  $2L_{search\ XT}$  by  
 463  $2L_{search\ AT}$  rectangle, centered on each reference point. Because the across-track location of the  
 464 repeat measurements for each reference point are determined by the errors in the repeat track  
 465 pointing of ATLAS, a data selection window centered on the RPT in the  $y$  direction will not  
 466 necessarily capture all of the available cycles of data. To improve the overlap between the  
 467 window and the data, we shift the reference point in the  $y$  direction so that the window includes  
 468 as many valid beam pairs as possible. We make this selection after the parameter-based (3.1.1)  
 469 and slope-based (3.1.2) editing steps because we want to maximize the number high-quality pairs  
 470 included, without letting the locations of low-quality segments influence our choice of the  
 471 reference-point shift.

472 We select the across-track offset for each reference point by searching a range of offset values,  $\delta$ ,  
 473 around the RPT to maximize the following metric:

$$M(\delta) = \frac{[\text{number of unique valid pairs entirely contained in } \delta \pm L_{search\ XT}] + [\text{number of unpaired segments contained in } \delta \pm L_{search\ XT}]/100}{2}$$

474 Maximizing this metric allows the maximum number of pairs with two valid segments to be  
 475 included in the fit, while also maximizing the number of segments included close to the center of  
 476 the fit. If multiple values of  $\delta$  have the same  $M$  value we choose the median of those  $\delta$  values.

477 The across-track coordinate of the adjusted reference point is then  $y_0 + \delta_{max}$ , where  $y_0$  is the  
 478 across-track coordinate of the unperturbed reference point. After this adjustment, the segments  
 479 in pairs that are contained entirely in the across-track interval  $\delta \pm L_{search\ XT}$  are identified as  
 480 *valid* based on the spatial search.

481 The location of the adjusted reference point is reported in the data group for each pair track, with  
 482 corresponding local coordinates in the *ref\_surf* subgroup: */ptx/ref\_surf/x\_atc*, */ptx/ref\_surf/y\_atc*.  
 483

### 484 3.2 Reference-Surface Shape Correction

485 To calculate the reference-surface shape correction, we construct the background surface shape  
 486 from valid segments selected during 3.1 and 3.2, using a least-squares inversion that separates  
 487 surface-shape information from elevation-change information. This produces surface shape-  
 488 corrected height estimates for cycles containing at least one valid pair, and a surface-shape  
 489 model that we use in later steps (3.4, 3.6) to calculate corrected heights for cycles that contain no  
 490 valid pairs and to calculate corrected heights for crossing tracks.



491 **3.2.1 Reference-surface shape inversion**

492 The reference-shape inversion solves for a reference surface and a set of corrected-height values  
 493 that represent the time-varying surface height at the reference point. The inversion involves  
 494 three matrices:

495 (i): a polynomial surface shape matrix, **S**, that describes the functional basis for the spatial part of  
 496 the inversion:

$$\mathbf{S} = \left[ \left( \frac{x - x_0}{l_0} \right)^p \left( \frac{y - y_0}{l_0} \right)^q \right] \quad 3$$

497 Here  $x_0$  and  $y_0$  are equal to the along-track coordinates of the adjusted reference point,  
 498 */ptx/ref\_surf/x\_atc* and */ptx/ref\_surf/y\_atc*, respectively. **S** has one column for each permutation  
 499 of  $p$  and  $q$  between zero and the degree of the surface polynomial in each dimension, but does  
 500 not include a  $p=q=0$  term. The degree in the along-track direction is chosen to be no more than  
 501 3 and no more than 1 less than the number of distinct  $x$  values in any cycle. The degree in the  
 502 across-track direction is chosen to be no more than 2 and to be no more than the number of  
 503 distinct pair-center  $y$  values, with the further (usually redundant) restriction that if the standard  
 504 deviation of selected pair  $y$  values is less than twice the across-track geolocation accuracy, the  
 505 across-track degree is no more than 1. For both components, distinct values are defined at a  
 506 resolution of 20 m. The scaling factor,  $l_0$ , ensures that the components of **S** are on the order of 1,  
 507 which improves the numerical accuracy of the computation. We set  $l_0=100$  m, to approximately  
 508 match the intra-pair beam spacing.

509 (ii): a matrix that encodes the repeat structure of the data, that accounts for the height-change  
 510 component of the inversion:

$$\mathbf{D} = [\delta(i, 1), \delta(i, 2), \dots, \delta(i, N)] \quad 4$$

511 Here  $\delta$  is the delta function, equal to 1 when its arguments are equal, zero otherwise, and  $i$  is an  
 512 index that increments by one for each distinct cycle in the selected data.

513 The surface shape and height time series are estimated by forming a composite design matrix, **G**,  
 514 where

$$\mathbf{G} = [\mathbf{S}, \mathbf{D}], \quad 5$$

515 and a covariance matrix, **C**, containing the squares of the segment-height error estimates on its  
 516 diagonal. The surface-shape polynomial and the height changes are found:

$$[\mathbf{s}, \mathbf{z}_c] = \mathbf{G}^{-g} \mathbf{z} \quad 6$$

$$\mathbf{G}^{-g} = [\mathbf{G}^T \mathbf{C}^{-1} \mathbf{G}]^{-1} \mathbf{G}^T \mathbf{C}^{-1}$$

517 The notation  $[\ ]^{-1}$  designates the inverse of the quantity in brackets, and  $\mathbf{z}$  is the vector of segment  
 518 heights. The parameters derived in this fit are  $\mathbf{s}$ , a vector of surface-shape polynomial  
 519 coefficients, and  $\mathbf{z}_c$ , a vector of corrected height values, giving the height at ( $lat_0, lon_0$ ) as  
 520 inferred from the height measurements and the surface polynomial. The matrix  $\mathbf{G}^{-g}$  is the  
 521 generalized inverse of **G**. The values of  $\mathbf{s}$  are reported in the *ref\_surf/poly\_ref\_surf* parameter, as  
 522 they are calculated from (6), with no correction made for the scaling in (3).

523 **3.2.2 Misfit analysis and iterative editing**

524 If blunders remain in the data input to the reference-surface calculation, they can lead to  
 525 inaccurate reference surfaces. To help remove these blunders, we iterate the inversion procedure  
 526 in 3.2.1, eliminating outlying data points based on their residuals to the reference surface.

527 To determine whether outliers may be present, we calculate the chi-squared misfit between the  
 528 data and the fit surface based on the data covariance matrix and the residual vector,  $r$ :

$$\chi^2 = r^T \mathbf{C}^{-1} r \quad 7$$

529 To determine whether this misfit statistic indicates consistency between the polynomial surface  
 530 and the data we use a P statistic, which gives the probability that the given  $\chi$  value would be  
 531 obtained from a random Gaussian distribution of data points with a covariance matrix  $\mathbf{C}$ . If the  
 532 probability is less than 0.025, we perform some further filtering/editing: we calculate the RDE of  
 533 the scaled residuals, eliminate any pairs containing a segment whose scaled residual magnitude is  
 534 larger than three times that value, and repeat the remaining segments.

535 After each iteration, any column of  $\mathbf{G}$  that has a uniform value (i.e. all the values are the same) is  
 536 eliminated from the calculation, and the corresponding value of the left-hand side of equation 7  
 537 is set to zero. Likewise, if the inverse problem has become less than overdetermined (i.e., the  
 538 number of data is smaller than the number of unknown values they are constraining), the  
 539 polynomial columns of  $\mathbf{G}$  are eliminated one by one until the number of data is greater than the  
 540 number of unknowns. Columns are eliminated in descending order of the sum of  $x$  and  $y$   
 541 degrees, and when there is a tie between columns based on this criterion, the column with the  
 542 larger  $y$  degree is eliminated first.

543 This fitting procedure is continued until no further segments are eliminated. If more than three  
 544 complete cycles that passed the initial editing steps are eliminated in this way, the surface is  
 545 assumed to be too complex for a simple polynomial approximation, and we proceed as follows:

546 (i) the fit and its statistics are reported based on the complete set of pairs that passed  
 547 the initial editing steps (valid pairs), using a planar ( $x$  degree =  $y$  degree = 1) fit in  $x$  and  $y$ .

548 (ii) the *ref\_surf/complex\_surface\_flag* is set to 1.

549 The misfit parameters are reported in the *ref\_surf* group: The final chi-squared statistic is  
 550 reported as *ref\_surf/misfit\_chi2r*, equal to the chi-squared statistic divided by the number of  
 551 degrees of freedom in the solution; the final RMS of the scaled residuals is reported as  
 552 *ref\_surf/misfit\_rms*.

553 **3.3 Reference-shape Correction Error Estimates**

554 We first calculate the errors in the corrected surface heights for segments included in the  
 555 reference-surface fit. We form a second covariance matrix,  $\mathbf{C}_1$ , whose diagonal elements are the  
 556 maximum of the squares of the segment errors and  $\langle r^2 \rangle$ . We estimate the covariance matrix for  
 557 the height estimates:

$$\mathbf{C}_m = \mathbf{G}^{-g} \mathbf{C}_1 \mathbf{G}^{-gT} \quad 8$$

558 The square roots of the diagonal values of  $\mathbf{C}_m$  give the estimated errors in the surface-polynomial  
 559 and height estimates due to short-spatial-scale errors in the segment heights. If there are  $N_{coeff}$   
 560 coefficients in the surface-shape polynomial, and  $N_{shape-cycles}$  cycles included in the surface-shape  
 561 fit, then the first  $N_{coeff}$  diagonal elements of  $\mathbf{C}_m$  give the square of the errors in the surface-shape  
 562 polynomial and the last  $N_{shape-cycles}$  give the errors in the surface heights for the cycles included in

563 the fit. The portion of  $C_m$  that refers only to the surface shape and surface-shape change  
 564 components is  $C_{m,s}$ .

### 565 3.4 Calculating corrected height values for repeats with no selected pairs

566 Once the surface polynomial has been established from the edited data set, corrected heights are  
 567 calculated for the unselected cycles (*i.e.* those from which all pairs were removed in the editing  
 568 steps): For the segments among these cycles, we form a new design matrix,  $S$  and multiply it by  
 569  $s$  to give the surface-shape correction:

$$z_c = z - Ss \quad 9$$

570 Here  $s$  is the surface-shape polynomial. This gives up to fourteen corrected-height values per  
 571 unselected cycle. From among these, we select the segment with the minimum error, as  
 572 calculated in the next step.

573 The height errors for segments from cycles not included in the surface-shape fit are calculated:

$$\sigma_{z,c}^2 = \text{diag}(SC_{m,s}S^T) + \sigma_z^2 \quad 10$$

574 Here  $\sigma_z$  is the error in the segment height, and  $\sigma_{z,c}$  is the error in the corrected height. The  
 575 results of these calculations give a height and a height error for each unselected segment. To  
 576 obtain a corrected elevation for each repeat that contains no selected pairs, we identify the  
 577 segment from that repeat that has the smallest error estimate, and report the value  $z_c$  as that  
 578 repeat's *ptx/h\_corr*, and use  $\sigma_{z,c}$  as its error (*/ptx/h\_corr\_sigma*).

### 579 3.5 Calculating systematic error estimates

580 The errors that have been calculated up to this point are due to errors in fitting segments to  
 581 photon-counting data and due to inaccuracies in the polynomial fitting model. Additional error  
 582 components can result from more systematic errors, such as errors in the position of ICESat-2 as  
 583 derived from POD, and pointing errors from PPD. These are estimated in the ATL06  
 584 *sigma\_geo\_xt*, *sigma\_geo\_at*, and *sigma\_geo\_r* parameters, and their average for each repeat is  
 585 reported in the *cycle\_stats* group under the same parameter names. The geolocation component  
 586 of the total height is the product of the geolocation error and the surface slope, added in  
 587 quadrature with the vertical height error:

$$\sigma_{h,systematic} = \left[ \left( \frac{dh}{dx} \sigma_{geo,AT} \right)^2 + \left( \frac{dh}{dy} \sigma_{geo,XT} \right)^2 + \sigma_{geo,r}^2 \right]^{1/2} \quad 11$$

588 For selected segments, which generally come from pairs containing two high-quality height  
 589 estimates,  $dh/dy$  is estimated from the ATL06 *dh\_fit\_dy* parameter. For unselected segments, it is  
 590 based on the  $y$  component of the reference-surface slope, as calculated in section 4.2.

591 The error for a single segment's corrected height is:

$$\sigma_{h,total} = [\sigma_{h,systematic}^2 + \sigma_{h,c}^2]^{1/2} \quad 12$$

592 This represents the total error in the surface height for a single corrected height. In most cases,  
 593 error estimates for averages of ice-sheet quantities will depend on errors from many segments  
 594 from different reference points, and the spatial scale of the different error components will need  
 595 to be taken into account in error propagation models. To allow users to separate these effects,  
 596 we report both the uncorrelated error, */ptx/h\_corr\_sigma*, and the component due only to  
 597 systematic errors, */ptx/h\_corr\_sigma\_systematic*. The total error is the quadratic sum of the two,  
 598 as described in equation 13.

599 **3.6 Calculating shape-corrected heights for crossing-track data**

600 Locations where groundtracks cross provide opportunities to check the accuracy of  
 601 measurements by comparing surface-height estimates between the groundtracks, and also offers  
 602 the opportunity to generate elevation-change time series that have more temporal detail than the  
 603 91-day repeat cycle can offer for repeat-track measurements.

604 At these crossover points, we use the reference surface calculated in 3.5 to calculate corrected  
 605 elevations for the crossing tracks. We refer to the track for which we have calculated the  
 606 reference surface as the *datum* track, and the other track as the *crossing* track. To calculate  
 607 corrected surface heights for the crossing ICESat-2 orbits, we first select all data from the  
 608 crossing orbit within a distance  $L\_search\_XT$  of the updated reference point on the datum track.  
 609 For most datum reference points, this will yield no crossing data, in which case the calculation  
 610 for that datum point terminates. If crossing data are found, we then calculate the coordinates of  
 611 these points in the reference point's along-track and across-track coordinates. This calculation  
 612 begins by transforming the crossing-track data into local northing and easting coordinates  
 613 relative to the datum reference-point location:

$$\delta N_c = \frac{\pi R_e}{180} (lat_c - lat_d) \tag{13}$$

$$\delta E_c = \frac{\pi R_e}{180} (lon_c - lon_d) \cos (lat_c)$$

614 Here  $(lat_d, lon_d)$  are the coordinates of the adjusted datum reference point,  $(lat_c, lon_c)$  are the  
 615 coordinates of the points on the crossing track, and  $R_e$  is the local radius of the WGS84 ellipsoid.  
 616 We then convert the northing and easting coordinates into along-track and across-track  
 617 coordinates based on the azimuth  $\phi$  of the datum track:

$$\begin{aligned} x_c &= \delta N_c \cos(\phi) + \delta E_c \sin(\phi) \\ y_c &= \delta N_c \sin(\phi) - \delta E_c \cos(\phi) \end{aligned} \tag{14}$$

618 Using these coordinates, we proceed as we did in 3.4 and 3.5: we generate  $S_k$  and  $S_{kt}$  matrices,  
 619 use them to correct the data and to identify the data point with the smallest error for each  
 620 crossing cycle. We report the time, error estimate, and corrected height for the minimum-error  
 621 datapoint from each cycle, as well as the location, pair, and track number corresponding to the  
 622 datum point in the */ptx/crossing\_track\_data* group. Because the crossing angles between the  
 623 tracks are oblique at high latitudes, a particular crossing track may appear in a few subsequent  
 624 datum points; in these cases, we expect that the error estimates should vary with the distance  
 625 between the crossing track and the datum track, so that the point with the minimum error should  
 626 correspond to the precise crossing location of the two tracks.

627 To help evaluate the quality of crossing-track data we calculate the *along\_track\_rss* parameter  
 628 for each crossing-track measurement. This parameter gives the RSS of the differences between  
 629 each segment's endpoint heights and the heights of the previous and subsequent segments. A  
 630 segment that is consistent with the previous and next segments in slope and elevation will have a  
 631 small value for this parameter, a segment that is inconsistent (and thus potentially in error) will  
 632 have a large value. Crossing-track measurements that have values greater than 10 m are  
 633 excluded from ATL11 and do not appear in the dataset.

634 **3.7 Calculating parameter averages**

635 ATL11 contains a variety of parameters that mirror parameters in ATL06, but are averaged to the  
 636 140-m ATL11 resolution. Except where noted otherwise, these quantities are weighted averages  
 637 of the corresponding ATL06 values. For selected pairs (i.e. those included in the reference-  
 638 surface fit), the parameters are averaged over the selected segments from each cycle, using  
 639 weights derived from their formal errors,  $h\_li\_sigma$ . The parameter weighted average for the  $N_k$   
 640 segments from cycle  $k$  is then:

$$\langle q \rangle = \frac{\sum_{i=1}^{N_k} |\sigma_i^{-2}| q_i}{\sum_{i=1}^{N_k} |\sigma_i^{-2}|} \quad 15$$

641 Here  $q_i$  are the parameter values for the segments. For repeats with no selected pairs, recall that  
 642 the corrected height for only one segment is reported in  $/ptx/h\_corr$ ; for these, we simply report  
 643 the corresponding parameter values for that selected segment.  
 644

645 **3.8 Output data editing**

646 The output data product includes cycle height estimates only for those cycles that have  
 647 non-systematic error estimates ( $/ptx/h\_corr\_sigma$ ) less than 15 m. All other heights (and their  
 648 errors) are reported as *invalid*.  
 649

650 **3.9 Antarctic geolocation biases**

651 As part of understanding apparent track-to-track variations in surface-height-change rates that we  
 652 had seen in the gridded products, we performed a crossover analysis of ATL06 data in Antarctica  
 653 and Greenland. This analysis showed that in the Antarctic data there are systematic spot-to-spot  
 654 elevation biases that vary on periods of a few months, but no corresponding bias variations in  
 655 Greenland. Analysis of the spot-to-spot pattern in these biases shows that they are consistent  
 656 with biases in the geolocation for the whole array, varying slowly in the along- and across-track  
 657 direction, which leads to height biases that are largest for the outlying spots in the array,  
 658 particularly at times when the array was pointed away from nadir. In release 6 of ATL11, these  
 659 biases are corrected, so that the Antarctic product shows a much smaller systematic height  
 660 variation between the left and right beam pairs. Expected maximum changes in reported surface  
 661 height are on the order of 3-5 cm in magnitude, opposite in sign between left and right beam  
 662 pairs. We have introduced the  $dh\_geoloc$  parameter to report the magnitude of the correction for  
 663 each reference point. This parameter is zero for all data except those collected in the Antarctic.

664 **3.9.1 Estimating Antarctic geolocation biases**

665 The relative displacement between the measured spot location and ICESat-2 is specified by the  
 666 segment azimuth,  $\phi_{sg}$ , the azimuth of the beam,  $\phi_{ref}$ , the surface height,  $h_{LI}$ , the elevation  
 667 angle of the satellite from each spot,  $\theta_{sat}$ , and the ~511-km height of ICESat-2 above the  
 668 reference ellipsoid ( $H_{sat}$ ). The vector from the satellite to each spot, in along-track coordinates,  
 669 is

$$\begin{aligned} & [x_{spot} \quad y_{spot} \quad dh_{surf-sat}] && 16 \\ & = [-\rho \cos(\phi_{seg} - \phi_{ref}) \quad -\rho \sin(\phi_{seg} - \phi_{ref}) \quad h_{li} - H_{sat}] \end{aligned}$$

670  
671 where

$$\rho = (H_{sat} - h_{LI}) \tan(\theta_{sat}).$$

672 The right triangle between the nadir point below the surface (x=y=0), the satellite, and the spot  
673 locations defines the relation between the spot location and the estimated surface height:

$$(H_{sat} - h_{surf})^2 + x_{spot}^2 + y_{spot}^2 = R^2 \quad 17$$

675 The differential of this equation with respect to  $h_{surf}$ ,  $x_{spot}$  and  $y_{spot}$  gives:

$$dh_{surf} = \frac{x_{spot}}{(H_{sat} - h_{surf})} \delta x_{spot} + \frac{y_{spot}}{(H_{sat} - h_{surf})} \delta y_{spot} \quad 18$$

677 This expresses the relation between errors in the x and y components of spot position and errors  
678 in the estimated surface height. At a crossover point, the estimated height difference between the  
679 two measurements will include an error component due to spot mislocation:

$$h_2 - h_1 = \left( \frac{x_{spot,2} - x_{spot,1}}{H_{sat} - h_{surf}} \right) \delta x_{spot} + \left( \frac{y_{spot,2} - y_{spot,1}}{H_{sat} - h_{surf}} \right) \delta y_{spot} \quad 19$$

680 Here we have ignored variations in apparent surface height due to temporal changes in the  
681 satellite and surface heights and the geolocation error between the two measurements. We can  
682 estimate the bias for a collection of crossover measurements by finding the values of  
683  $\delta x_{spot}$ ,  $\delta y_{spot}$  that minimize the quantity:

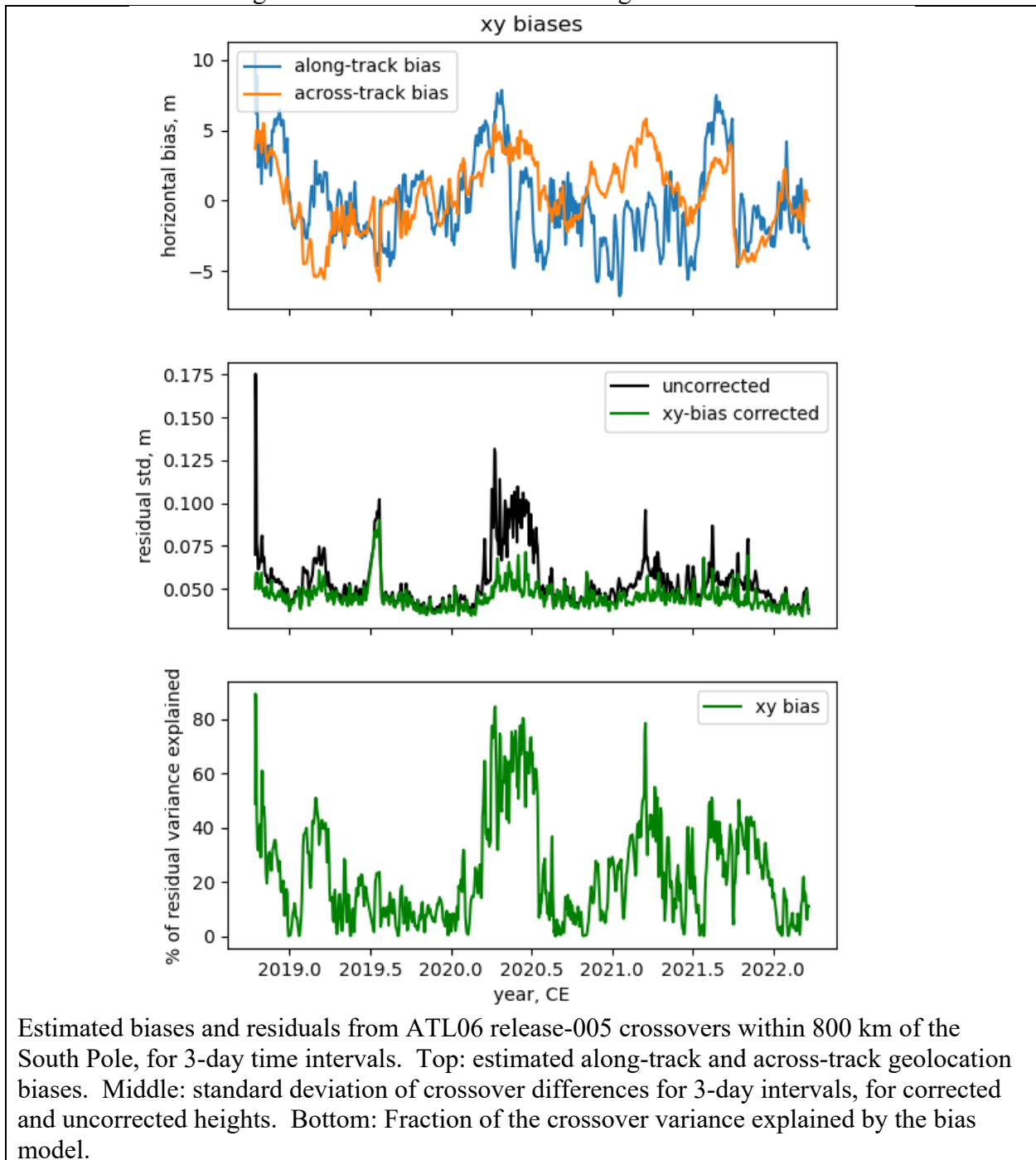
$$\begin{aligned} & \sum_{i,j \in \text{crossovers}} \left[ (h_j - h_i) - \left( \frac{x_{spot,j} - x_{spot,i}}{H_{sat} - h_{surf}} \right) \delta x_{spot} \right. && 20 \\ & \left. + \left( \frac{y_{spot,j} - y_{spot,i}}{H_{sat} - h_{surf}} \right) \delta y_{spot} \right]^2 \end{aligned}$$

685 We derive a time series of  $\delta x_{spot}$ ,  $\delta y_{spot}$  by minimizing [] for collections of crossovers chosen  
686 so that both measurements in the crossover fall within short (3-day) intervals, spaced regularly  
687 (every 1.5 days) throughout the mission. We apply an iterated three-sigma edit as part of the  
688 fitting process to avoid letting outlying values in the height-difference distribution influence the  
689 recovered value.

691

692

Figure 3-3. Correction for Antarctic geolocation biases



693

694 Figure 3.3 shows the estimated x and y biases for Antarctic crossovers measured for the interior  
 695 of the ice sheet (within 800 km of the Antarctic pole hole) for cycles 1-15 of the mission, as well  
 696 time series of RMS crossover differences as a function of time, both before and after the  
 697 correction is applied, and the fraction of crossover-difference variance explained by the

698 correction. Over most of the mission, the biases vary between -5 m and +5 m in each direction,  
 699 with occasional excursions as large as 7 m. The uncorrected crossovers have standard deviations  
 700 as large as 0.1 m, most consistently in a 3-4 month period in early 2020. Correcting for the  
 701 biases reduces the crossover standard deviations to the 0.04-0.05 m range, except for the July-  
 702 2019 period affected by the observatory safe hold, when the residuals remain large, at 0.07-0.1  
 703 m. The correction for the geolocation bias accounts for 10-80% of the total crossover-difference  
 704 variance over most of the mission.

705 To demonstrate the structure of the errors related to the geolocation biases, we plot the  
 706 statistics of corrected crossovers using data collected between 1000 and 1800 km from the south  
 707 pole, at surface elevations greater than 1800m. This is a set of data distinct from that used to  
 708 generate the bias estimates and includes high-elevation parts of Antarctica where surface-height  
 709 changes should be small and surface slopes should be small. In figure 3-4, We plot four time  
 710 series of RMS crossover differences: crossovers where both measurements come from the same  
 711 beam pair, for crossovers where one measurement comes from a center pair and the other where  
 712 the comes from an edge pair, and for crossovers where the measurements come from different  
 713 edge pairs. These plots show that in the uncorrected data, the RMS differences follow a  
 714 consistent order, smallest for those with both measurements from the same spot, and, in  
 715 increasing order, those from the same pair but different spots, differences between the center pair  
 716 and edge pair, and differences between different edge pairs. This matches the expected relation,  
 717 where the farther apart two spots are in the array, the larger the difference between their biases  
 718 should be. Correcting for the geolocation errors using the biases estimated from the data close to  
 719 the polehole (plotted in figure 3.3) yields crossover differences with approximately equal RMS  
 720 values for all combinations of spots, with typical RMS values between 0.04 and 0.05 m. These  
 721 statistics suggest that the biases calculated using the polehole data are representative of biases  
 722 over the rest of Antarctica, and that correcting for these biases makes a significant improvement  
 723 in height-estimate accuracy, particularly for the edge beam pairs.

### 724 3.9.2 Correcting for Antarctic geolocation biases.

725  
 726 As part of routine data operations for ATL06 production, we generate crossovers for Antarctica.  
 727 We generate a new set of xy-bias estimates each time a new set of ATL06 data are delivered  
 728 from SIPS, which are stored as a comma-separated-value file, called, for example:

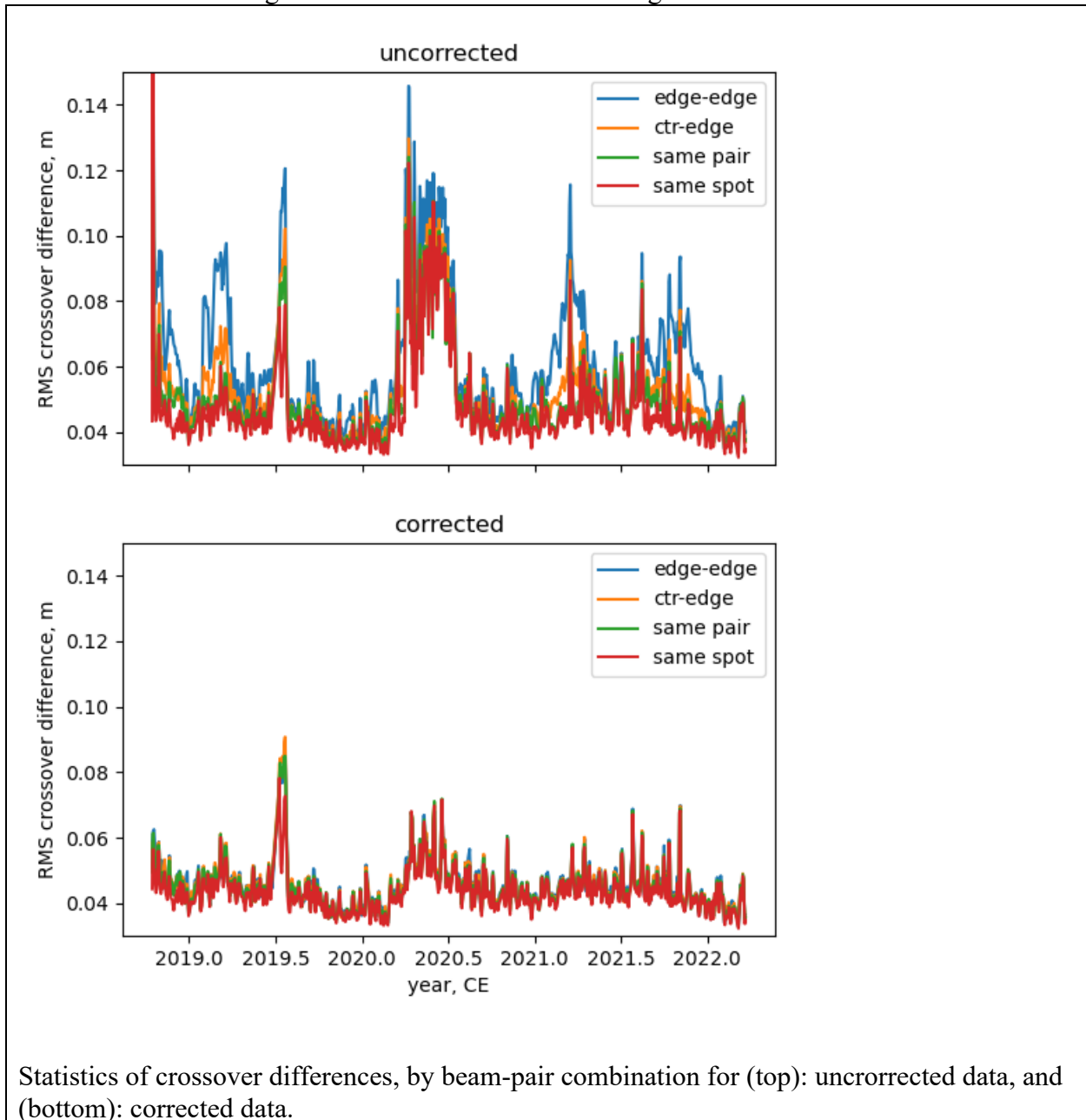
729 `xy_geoloc_bias_est_AA_800km_3day_20221208.csv`

730 Here AA\_800km indicates that the crossovers were generated for Antarctica, for data within 800  
 731 km of the polehole, \_3day\_ indicates the temporal resolution of the time series, and 20221208  
 732 indicates that the file was generated on December 12 2022.

733  
 734 We correct for the errors in the spot geolocation by calculating a value of  $\delta x_{spot}$ ,  $\delta y_{spot}$  for each  
 735 ATL06 measurement by linear interpolation into the time series stored in the csv file. We then  
 736 use equation [???] to calculate the height error for each measurement and subtract it from that  
 737 measurement's  $h_{li}$  value, and adjust the  $x_{atc}$ ,  $y_{atc}$ , values by adding the interpolated  
 738  $\delta x_{spot}$ ,  $\delta y_{spot}$  values to each. We do not make adjustments to the geolocation values (i.e.  
 739 latitude and longitude) in the data, because the most significant effect of the geolocation for the  
 740



Figure 3-4. Correction for Antarctic geolocation biases



Statistics of crossover differences, by beam-pair combination for (top): uncorrected data, and (bottom): corrected data.

741 points affects the relative position of the measurements, which is accounted for by shifting the  
 742 points in along-track coordinates. The mean vertical geolocation correction for each cycle, pair  
 743 and reference point is stored in the `/ptx/cycle_stats/dh_geoloc` parameter.  
 744

## 745 4.0 LAND ICE PRODUCTS: LAND ICE H (T)(ATL 11/L3B)

746 Each ATL11 file contains data for a single reference ground track, for one of the subregions  
 747 defined for ATLAS granules (see Figure 6-3). The ATL11 consists of three top-level groups, one  
 748 for each beam pair (*pt1*, *pt2*, *pt3*). Within each pair-track group, there are datasets that give the  
 749 corrected heights for each cycle, their errors, and the reference-point locations. Subgroups  
 750 (*cycle\_stats*, and *ref\_surf*) provide a set of data-quality parameters, and ancillary data describing  
 751 the fitting process, and use the same ordering and coordinates as the top-level group (i.e. any  
 752 dataset within the */ptx/cycle\_stats* and */ptx/ref\_surf* groups refers to the same latitude, longitude,  
 753 and reference points as the corresponding measurements in the */ptx/* groups.) The  
 754 *crossing\_track\_data* group gives height measurements at crossover locations, and has its own set  
 755 of locations and essential ATL06-derived parameters.  
 756

### 757 4.1 File naming convention

758 ATL11 files are named in the following format:

759 `ATL11_ttttgg_cccc_rrr_vv.h5`

760 Here *tttt* is the rgt number, *gg* is the granule-region number, *cccc* gives the first and last cycles of  
 761 along-track data included in the file (e.g. `_0308_` would indicate that cycles three through eight,  
 762 inclusive, might be included in the along-track solution), and *rrr* is the release number. and *vv* is  
 763 the version number, which is set to one the first time a granule is generated for a given data  
 764 release, and is incremented by one if the granule is regenerated.  
 765

### 766 4.2 */ptx* group

767

768 Table 4-1 shows the datasets in the *ptx* groups. This group gives the principal output parameters  
 769 of the ATL11. The corrected repeat measurements are in */ptx/h\_corr*, which gives improved  
 770 height measurements based on a surface fit to valid data at paired segments. The associated  
 771 reference coordinates, */ptx/latitude* and */ptx/longitude* give the reference point location, with  
 772 averaged times per repeat, */ptx/delta\_time*. For repeats with no selected pairs, the corrected  
 773 height is that from the selected segment with the lowest error. Two error metrics are given in  
 774 */ptx/h\_corr\_sigma* and */ptx/h\_corr\_sigma\_systematic*. The first gives the error component due to  
 775 ATL06 range errors and due to uncertainty in the reference surface. The second gives the  
 776 component due to geolocation and radial-orbit errors that are correlated at scales larger than one  
 777 reference point; adding these values in quadrature gives the total per-cycle error. Values are only  
 778 reported for */ptx/h\_corr*, */ptx/h\_corr\_sigma*, and */ptx/h\_corr\_sigma\_systematic* for those cycles  
 779 whose uncorrelated errors are less than 15 m; all others are reported as *invalid*. A  
 780 */ptx/quality\_summary* is included for each cycle, based on fit statistics from ATL06.

781

782

**Table 4-1 Parameters in the /ptx/ group**

Parameter	Units	Dimensions	Description
<i>cycle_number</i>	counts	$I \times N_{cycles}$	Cycle number for each column of the data
<i>latitude</i>	degrees North	$N_{pts} \times I$	Reference point latitude
<i>longitude</i>	degrees East	$N_{pts} \times I$	Reference point longitude
<i>ref_pt</i>	counts	$N_{pts} \times I$	The reference point number, <i>m</i> , counted from the equator crossing of the RGT.
<i>delta_time</i>	seconds	$N_{pts} \times N_{cycles}$	mean GPS time for the segments for each cycle
<i>h_corr</i>	meters	$N_{pts} \times N_{cycles}$	the mean corrected height
<i>h_corr_sigma</i>	meters	$N_{pts} \times N_{cycles}$	the formal error in the corrected height
<i>h_corr_sigma_systematic</i>	meters	$N_{pts} \times N_{cycles}$	the magnitude of the RSS of all errors that might be correlated at scales larger than a single reference point (e.g. pointing errors, GPS errors, etc)
<i>quality_summary</i>	counts	$N_{pts} \times N_{cycles}$	summary flag: zero indicates high-quality cycles: where $\min(\text{signal\_selection\_source}) \leq 1$ and $\min(\text{SNR\_significance}) < 0.02$ , and $\text{ATL06\_summary\_zero\_count} > 0$ .

783

784 **4.3 /ptx/ref\_surf group**

785 Table 4-2 describes the /ptx/ref\_surf group. This group includes parameters describing the  
 786 reference surface fit at each reference point. The polynomial coefficients are given in  
 787 /ptx/poly\_ref\_surf, sorted first by total degree, then by x-component degree. Because the

788 polynomial degree is chosen separately for each reference point, enough columns are provided in  
 789 the */ptx/poly\_ref\_surf* and */ptx/poly\_ref\_surf\_sigma* to accommodate all possible components up  
 790 to 2<sup>rd</sup> degree in *y* and 3<sup>th</sup> degree in *x*, and absent values are filled in with zeros. The  
 791 correspondence between the columns of the polynomial fields and the exponents of the *x* and *y*  
 792 terms are given in the */ptx/poly\_exponent\_x* and */ptx/poly\_exponent\_y* fields.

**Table 4-2 Parameters in the */ptx/ref\_surf* group**

Parameter	Units	Dimensions	Description
<i>dem_h</i>	Meters	$N_{pts} \times 1$	DEM elevation, derived from the ATL06 <i>dem_h</i> parameter
<i>geoid_h</i>	Meters	$N_{pts} \times 1$	Geoid height above WGS-84 reference ellipsoid in the tide-free system, derived from ATL06 <i>/gtxx/atl06_segments/dem/geoid_h</i>
<i>complex_surface_flag</i>	counts	$N_{pts} \times 1$	0 indicates that normal fitting was attempted, 1 indicates that the signal selection algorithm rejected too many repeats, and only a linear fit was attempted
<i>rms_slope_fit</i>	counts	$N_{pts} \times 1$	the RMS of the slope of the fit polynomial within 50 m of the reference point
<i>e_slope</i>	counts	$N_{pts} \times 1$	the mean East-component slope for the reference surface within 50 m of the reference point
<i>n_slope</i>	counts	$N_{pts} \times 1$	the mean North-component slope for the reference surface within 50 m of the reference point
<i>at_slope</i>	Counts	$N_{pts} \times 1$	Mean along-track component of the slope of the reference surface within 50 m of the reference point
<i>xt_slope</i>		$N_{pts} \times 1$	Mean across-track component of the slope of the reference surface within 50 m of the reference point
<i>deg_x</i>	counts	$N_{pts} \times 1$	Maximum degree of non-zero polynomial components in <i>x</i>
<i>deg_y</i>	counts	$N_{pts} \times 1$	Maximum degree of non-zero polynomial components in <i>y</i>
<i>poly_exponent_x</i>	counts	$1 \times 8$	Exponents for the <i>x</i> factors in the surface polynomial
<i>poly_exponent_y</i>	counts	$1 \times 8$	Exponents for the <i>y</i> factors in the surface polynomial
<i>poly_coeffs</i>	counts	$N_{pts} \times 8$	polynomial coefficients (up to degree 3), for polynomial components scaled by 100 m
<i>poly_ref_coefs_sigma</i>	counts	$N_{pts} \times 8$	formal errors for the polynomial coefficients

<i>ref_pt_number</i>	counts	$N_{pts} \times I$	Ref point number, counted from the equator crossing along the RGT.
<i>x_atc</i>	meters	$N_{pts} \times I$	Along-track coordinate of the reference point, measured along the RGT from its first equator crossing.
<i>y_atc</i>	meters	$N_{pts} \times I$	Across-track coordinate of the reference point, measured along the RGT from its first equator crossing.
<i>rgt_azimuth</i>	degrees	$N_{pts} \times I$	Reference track azimuth, in degrees east of local north
<i>misfit_chi2r</i>	meters	$N_{pts} \times I$	misfit chi square, divided by the number of degrees in the solution
<i>misfit_rms</i>	meters	$N_{pts} \times I$	RMS misfit for the surface-polynomial fit
<i>fit_quality</i>	counts	$N_{pts} \times I$	Indicates quality of the fit: 0: no problem identified 1: One or more polynomial coefficient errors larger than 10 2: One or more components of the surface slope has magnitude larger than 0.2 3: Conditions 1 and 2 both true.

793

794

795 The slope of the fit surface is given in the *ref\_surf/n\_slope* and *ref\_surf/e\_slope* parameters in  
796 the local north and east directions; the corresponding slopes in the along-track and across-track  
797 directions are given in the *ref\_surf/xt\_slope* and *ref\_surf/yt\_slope* parameters. For the along-  
798 track points, the surface slope is calculated by evaluating the correction-surface polynomial for a  
799 10-m spaced grid of points extending  $\pm 50$  m in  $x$  and  $y$  around the reference point, and  
800 calculating the mean slopes of these points. The calculation is performed in along-track  
801 coordinates and then projected onto the local north and east vectors. The *rms\_slope\_fit* is  
802 derived from the same set of points, and is calculated as the RMS of the standard deviations of  
803 the slopes calculated from adjacent grid points, in  $x$  and  $y$ .

804

#### 805 4.4 /ptx/cycle\_stats group

806 The /ptx/cycle\_stats group gives summary information about the segments present for each  
807 reference point. Most parameters are averaged according to equation 14, but for others (e.g.

808 /ptx/signal\_selection\_flag\_best, which is the minimum of the signal selection flags for the cycle)  
 809 **Table 4-3** describes how the summary statistics are derived.

810

811 **Table 4-3 Parameters in the /ptx/cycle\_stats group**

Parameter	Units	Dimensions	Description
<i>ATL06_summary_zero_count</i>	counts	$N_{pts} \times N_{cycles}$	Number of segments with <i>atl06_quality_summary</i> =0 (0 indicates the best-quality data)
<i>h_rms_misfit</i>	meters	$N_{pts} \times N_{cycles}$	Weighted-average RMS misfit between PE heights and along-track land-ice segment fit
<i>dh_geoloc</i>	meters	$N_{pts} \times N_{cycles}$	Correction applied to Antarctic heights based on estimates of the geolocation bias.
<i>r_eff</i>	counts	$N_{pts} \times N_{cycles}$	Weighted-average effective, uncorrected reflectance for each cycle.
<i>tide_ocean</i>	meters	$N_{pts} \times N_{cycles}$	Weighted-average ocean tide for each cycle
<i>dac</i>	meters	$N_{pts} \times N_{cycles}$	Dynamic atmosphere correction (mainly the effect of atmospheric pressure on floating-ice elevation).
<i>cloud_flg_atm</i>	counts	$N_{pts} \times N_{cycles}$	Minimum cloud flag from ATL06: Flag indicates confidence that clouds with $OT^* > 0.2$ are present in the lower 3 km of the atmosphere based on ATL09
<i>cloud_flg_asr</i>	counts	$N_{pts} \times N_{cycles}$	Minimum apparent-surface-reflectance - based cloud flag from ATL06: Flag indicates confidence that clouds with $OT > 0.2$ are present in the lower 3 km of the atmosphere based on ATL09
<i>bsnow_h</i>	meters	$N_{pts} \times N_{cycles}$	Weighted-average blowing snow layer height for each cycle
<i>bsnow_conf</i>	counts	$N_{pts} \times N_{cycles}$	Maximum <i>bsnow_conf</i> flag from ATL06: indicates the greatest (among segments) confidence flag for presence of blowing snow for each cycle

Parameter	Units	Dimensions	Description
<i>x_atc</i>	meters	$N_{pts} \times N_{cycles}$	weighted average of pair-center RGT y coordinates for each cycle
<i>y_atc</i>	meters	$N_{pts} \times N_{cycles}$	weighted mean of pair-center RGT y coordinates for each cycle
<i>ref_pt</i>		$N_{pts} \times N_{cycles}$	Ref point number, counted from the equator crossing along the RGT.
<i>seg_count</i>	counts	$N_{pts} \times N_{cycles}$	Number of segments marked as valid for each cycle. Equal to 0 for those cycles not included in the reference-surface shape fit.
<i>min_signal_selection_source</i>	counts	$N_{pts} \times N_{cycles}$	Minimum of the ATL06 <i>signal_selection_source</i> value (indicates the highest-quality segment in the cycle)
<i>min_snr_significance</i>	counts	$N_{pts} \times N_{cycles}$	Minimum of <i>SNR_significance</i> (indicates the quality of the best segment in the cycle)
<i>sigma_geo_h</i>	meters	$N_{pts} \times N_{cycles}$	Root-mean-weighted-square-average total vertical geolocation error due to PPD and POD
<i>sigma_geo_at</i>	meters	$N_{pts} \times N_{cycles}$	Root-mean-weighted-square-average local-coordinate x horizontal geolocation error for each cycle due to PPD and POD
<i>sigma_geo_xt</i>	meters	$N_{pts} \times N_{cycles}$	Root-mean-weighted-square-average local-coordinate y horizontal geolocation error for each cycle due to PPD and POD
<i>h_mean</i>	meters	$N_{pts} \times N_{cycles}$	Weighted-average of surface heights, not including the correction for the reference surface

812 \*OT (optical thickness) is a measure of signal attenuation used in atmospheric calculations. This  
 813 parameter discussed in ICESat-2 atmospheric products (ATL09)  
 814

#### 815 4.5 /ptx/crossing\_track\_data group

816 The /ptx/crossing\_track\_data group (Table 4-4) contains elevation data at crossover locations.  
 817 These are locations where two ICESat-2 pair tracks cross, so data are available from both the  
 818 datum track, for which the granule was generated, and from the crossing track. The data in this  
 819 group represent the elevations and times from the crossing tracks, corrected using the reference

820 surface from the datum track. Each set of values gives the data from a single segment on the  
821 crossing track, that was selected as having the minimum error among all segments on the  
822 crossing track within the  $2 L\_search\_XT$ –by- $2 L\_search\_AT$  window around the reference point  
823 on the datum track. The systematic errors are evaluated based on the magnitude of the reference-  
824 surface slope and the magnitude of the horizontal geolocation error of the crossing-track data.  
825 Attributes for the group specify the track number and pair-track number of the crossing track.  
826



827

**Table 4-4 Parameters in the /ptx/crossing\_track\_data group**

Parameter	Units	Dimensions	Description
<i>ref_pt</i>	counts	$N_{XO} \times 1$	the reference-point number for the datum track
<i>delta_time</i>	years	$N_{XO} \times 1$	time relative to the ICESat-2 reference epoch
<i>dh_geoloc</i>	meters	$N_{XO} \times 1$	Correction applied to Antarctic heights based on estimates of the geolocation bias.
<i>h_corr</i>	meters	$N_{XO} \times 1$	WGS-84 height, corrected for the ATL11 surface shape
<i>h_corr_sigma</i>	meters	$N_{XO} \times 1$	error in the height estimate
<i>h_corr_sigma_systematic</i>	meters	$N_{XO} \times 1$	systematic error in the height estimate
<i>ocean_tide</i>	Meters	$N_{XO} \times 1$	Ocean-tide estimate for the crossing track
<i>dac</i>	Meters	$N_{XO} \times 1$	Dynamic atmosphere correction for the crossing track
<i>latitude</i>	degrees	$N_{XO} \times 1$	latitude of the crossover point
<i>longitude</i>	degrees	$N_{XO} \times 1$	longitude of the crossover point
<i>cycle_number</i>	counts	$N_{XO} \times 1$	Cycle number for the crossing data
<i>rgt</i>	counts	$N_{XO} \times 1$	The RGT number for the crossing data
<i>spot_crossing</i>	counts	$N_{XO} \times 1$	The spot number for the crossing data
<i>atl06_quality_summary</i>	counts	$N_{XO} \times 1$	quality flag for the crossing data derived from ATL06. 0 indicates no problems detected, 1 indicates potential problems
<i>along_track_rss</i>	meters	$N_{XO} \times 1$	Root sum of the squared differences between the heights of the endpoints for the crossing-track segment and the centers of the previous and next segments

828

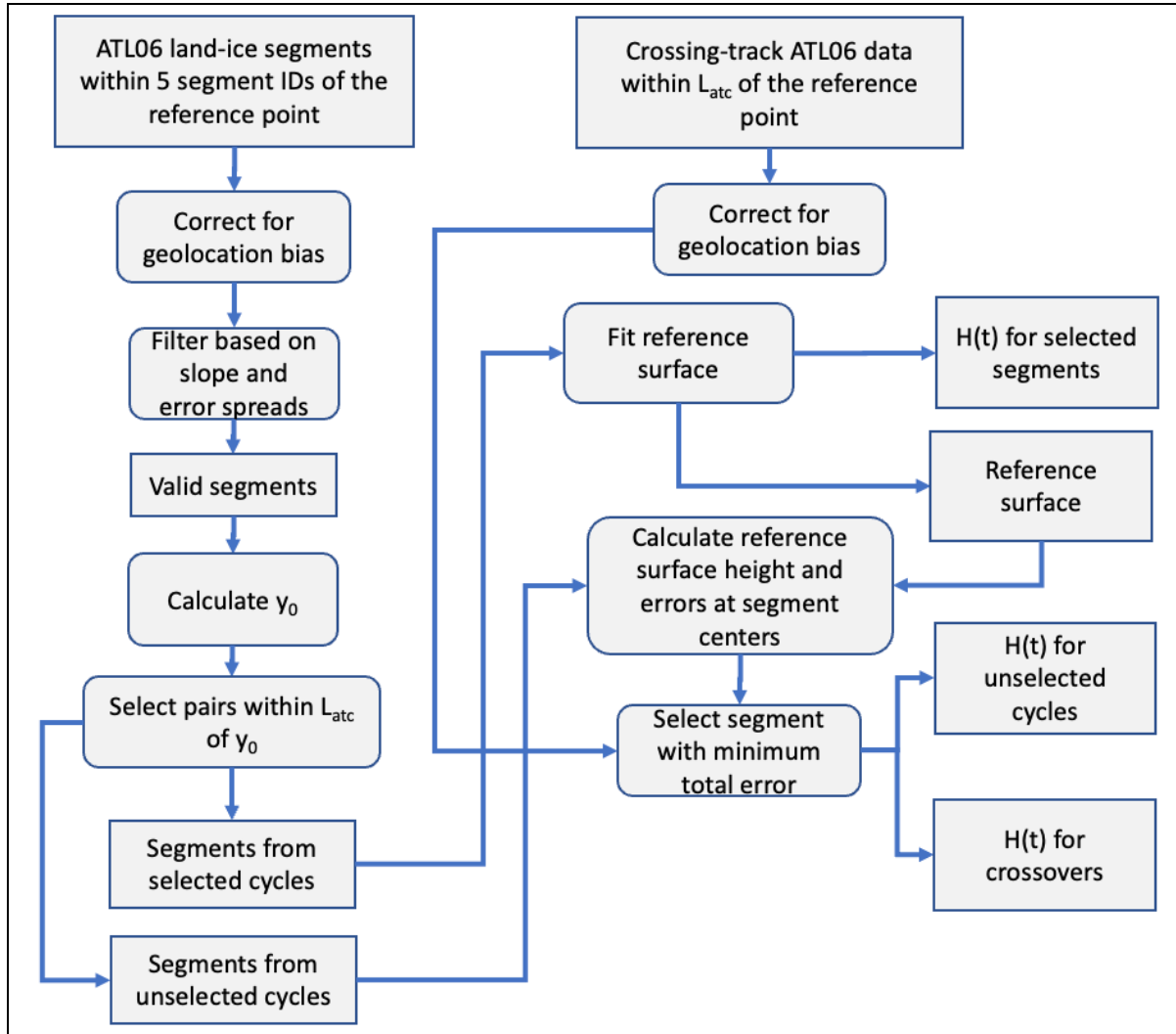
829

830 5.0 ALGORITHM IMPLEMENTATION

831

832

Figure 5-1 Flow Chart for ATL11 Surface-shape Corrections



833

834

835 The following steps are performed for each along-track reference point.

- 836 1. Segments with *segment\_id* within  $N\_search/2$  of the reference-point number, are
- 837 selected.
- 838 2. Valid segments are identified based on estimated errors, the *ATL06\_quality\_summary*
- 839 parameter, and the along- and across-track segment slopes. Valid pairs, containing valid
- 840 measurements from two different beams, are also identified.
- 841 3. The location of the reference point is adjusted to allow the maximum number of repeats
- 842 with at least one valid pair to fall within the across-track search distance of the reference
- 843 point.

- 844 4. The reference surface is fit to pairs with two valid measurements within the search  
 845 distance of the reference point. This calculation also produces corrected heights for the  
 846 selected pairs and the errors in the correction polynomial coefficients.  
 847 5. The correction surface is used to derive corrected heights for segments not selected in  
 848 steps 1-3, and the height for the segment with the smallest error is selected for each  
 849 6. The reference surface is used to calculate heights for external (pre-ICESat-2) laser  
 850 altimetry data sets and crossover ICESat-2 data.  
 851 A schematic of this calculation is shown in Figure 5-1.

### 852 5.1.1 Select ATL06 data for the current reference point

853 **Inputs:**

- 854 *ref\_pt*: segment number for the current reference point  
 855 *track\_num*: The track number for current point  
 856 *pair\_num*: The pair number for the current point  
 857 *along\_track\_shift\_table*: Estimated geolocation bias lookup table (delta x, y atc vs. delta time)

858 **Outputs:**

- 859 *D\_ATL06*: ATL06 data structure

860 **Parameters:**

- 861 *N\_search*: number of segments to search, around *ref\_pt*, equal to 5.

862 **Algorithm:**

- 863 1. For each along-track point, load all ATL06 data from track *track\_num* and pair *pair\_num* that  
 864 have *segment\_id* within *N\_search* of *ref\_pt*: These segments have  $ref\_pt - N\_search$   
 865  $\leq segment\_id \leq ref\_pt + N\_search$ .  
 866 2. Reject any data that have *y\_atc* values more than 500 m distant from the nominal pair-track  
 867 centers (3200 m for pair 1, 0 m for pair 2, -3200 m for pair 3).  
 868 Steps 3, 4, and 5 are only carried out for Antarctic data (for Arctic data, *along\_track\_shift\_table*  
 869 is not specified)  
 870 3. Calculate *x\_spot* and *y\_spot* using equation 17, assuming that the satellite elevation above the  
 871 ellipsoid is 511 km  
 872 4. Interpolate *delta\_x\_ATC* and *delta\_y\_ATC* from *along\_track\_shift\_table* as a function of time.  
 873 5. Calculate the corrected height using equation 19. Assign the difference between the corrected  
 874 height and the uncorrected height to the *dh\_geoloc* variable in the ATL06 data structure.  
 875 6. Subtract *delta\_x\_ATC* and *delta\_y\_ATC* from the *x\_atc* and *y\_atc* variables in the ATL06  
 876 data structure.  
 877

### 878 5.1.2 Select pairs for the reference-surface calculation

879 **Inputs:**

- 880 *ref\_pt*: reference point number for the current fit  
 881 *x\_atc\_ctr*: Along-track coordinate of the reference point  
 882 *D\_ATL06*: ATL06 data structure  
 883 *pair\_data*: Structure describing ATL06 pairs, includes mean of strong/weak beam *y\_atc* and  
 884 *dh\_fit\_dy*

885 **Outputs:**

886 **validity flags for each segment:**

887 *valid\_segs.x\_slope*: Segments identified as valid based on x-slope consistency  
 888 *valid\_segs.data*: Segments identified as valid based on ATL06 parameter values.

889 **Validity flags for each pair:**

890 *valid\_pairs*: Pairs selected for the reference-surface calculation  
 891 *valid\_pairs.y\_slope*: Pairs identified as valid based on y-slope consistency  
 892 *y\_polyfit\_ctr*: y center of the slope regression  
 893 *ref\_surf/complex\_surface\_flag*: Flag indicating 0: non-complex surface, 1: complex surface.

894

895 **Parameters:**

896 *L\_search\_XT*: The across-track search distance.  
 897 *N\_search*: Along-track segment search distance  
 898 *seg\_sigma\_threshold\_min*: Minimum threshold for accepting errors in segment heights, equal to  
 899 0.05 m.

900 **Algorithm:**

901 1. Flag valid segments based on ATL06 values.

902 1a. Count the cycles that contain at least one pair that has *atl06\_quality\_flag*=0  
 903 for both segments. If this number is greater than  $N\_cycles/3$ , set  
 904 *ref\_surf/complex\_surface\_flag*=0 and set *valid\_segs.data* to 1 for segments with  
 905 *ATL06\_quality\_summary* equal to 0. Otherwise, set *ref\_surf/complex\_surface\_flag*=1 and set  
 906 *valid\_segs.data* to 1 for segments with *snr\_significance* < 0.02.

907 1b. Define *seg\_sigma\_threshold* as the maximum of 0.05 or three times the median of  
 908 *sigma\_h\_li* for segments with *valid\_segs.data* equal to 1. Set *valid\_segs.data* to 1 for segments  
 909 with *h\_sigma\_li* less than this threshold and *ATL06\_quality\_summary* equal to 0.

910 1c. Define *valid\_pairs.data*: For each pair of segments, set *valid\_pairs.data* to 1 when  
 911 both segments are marked as valid in *valid\_segs.data*.

912 2. Calculate representative values for the x and y coordinate for each pair, and filter by distance.

913 2a. For each pair containing two defined values, set *pair\_data.x* to the segments' *x\_atc*  
 914 value, and *pair\_data.y* to the mean of the segments' *y\_atc* values.

915 2b. Calculate *y\_polyfit\_ctr*, equal to the median of *pair\_data.y* for pairs marked valid in  
 916 *valid\_pairs.data*.

917 2c. Set *valid\_pairs.ysearch* to 1 for pairs with  $|pair\_data.y - y\_polyfit\_ctr| <$

918 *L\_search\_XT*.

919 3. Select pairs based on across-track slope consistency

920 3a. Define *pairs\_valid\_for\_y\_fit*, for the across-track slope regression if they are marked  
 921 as valid in *valid\_pairs.data*, and *valid\_pairs.ysearch*, not otherwise.

922 3b. Choose the degree of the regression for across-track slope

923 -If the valid pairs contain at least two different *x\_atc* values (separated by at least  
 924 18 m), set the along-track degree, *my\_regression\_y\_degree*, to 1, 0 otherwise.

925 -If valid pairs contain at least two different *ref\_surf/y\_atc* values (separated by at  
 926 least 18 m), set the across-track degree, *my\_regression\_y\_degree*, to 1, 0 otherwise.

927 3c. Calculate the formal error in the y slope estimates: *y\_slope\_sigma* is the RSS of the  
 928 *h\_li\_sigma* values for the two beams in the pair divided by the difference in their *y\_atc*  
 929 values. Based on these, calculate *my\_regression\_tol*, equal to the maximum of 0.01 or three  
 930 times the median of *y\_slope\_sigma* for valid pairs (*pairs\_valid\_for\_y\_fit*).

931           3d. Calculate the regression of  $dh\_fit\_dy$  against  $pair\_data.x$  and  $pair\_data.y$  for valid  
932 pairs ( $pairs\_valid\_for\_y\_fit$ ). The result is  $y\_slope\_model$ , which gives the variation of  $dh\_fit\_dy$   
933 as a function of  $x\_atc$  and  $y\_atc$ . Calculate  $y\_slope\_resid$ , the residuals between the  $dh\_fit\_dy$   
934 values and  $y\_slope\_model$  for all pairs in  $pair\_data$ .

935           3e. Calculate  $y\_slope\_threshold$ , equal to the maximum of  $my\_regression\_tol$  and three  
936 times the RDE of  $y\_slope\_resid$  for valid pairs.

937           3f. Mark all pairs with  $|y\_slope\_resid| > y\_slope\_threshold$  as invalid. Re-establish  
938  $pairs\_valid\_for\_y\_fit$  (based on  $valid\_pairs.data$ ,  $valid\_pairs.y\_slope$  and  $valid\_pairs.ysearch$ ).  
939 Return to step 3d (allow two iterations total).

940           3g. After the second repetition of 3d-f, use the model to mark all pairs with  
941  $|y\_slope\_resid|$  less than  $y\_slope\_threshold$  with 1 in  $valid\_pairs.y\_slope$ , 0 otherwise.

942           4. Select segments based on along-track slope consistency for both segments in the pair

943           4a. Define  $pairs\_valid\_for\_x\_fit$ , valid segments for the along-track slope regression:  
944 segments are valid if they come from pairs marked as valid in  $valid\_pairs.data$  and  
945  $valid\_pairs.ysearch$ , not otherwise.

946           4b. Choose the degree of the regression for along-track slope  
947                -If valid segments contain at least two different  $x\_atc$  values set the along-track  
948 degree,  $mx\_regression\_x\_degree$ , to 1, 0 otherwise.

949                -If valid segments contain at least two different  $y\_atc$  values, set the across-track  
950 degree,  $mx\_regression\_y\_degree$ , to 1, 0 otherwise.

951           4c. Calculate along-track slope regression tolerance,  $mx\_regression\_tol$ , equal to the  
952 maximum of either 0.01 or three times the median of the  $dh\_fit\_dx\_sigma$  values for the valid  
953 pairs.

954           4d. Calculate the regression of  $dh\_fit\_dx$  against  $pair\_data.x$  and  $pair\_data.y$  for valid  
955 segments ( $pairs\_valid\_for\_x\_fit$ ). The result is  $x\_slope\_model$ , which gives the variation of  
956  $dh\_fit\_dx$  as a function of  $pair\_data.x$  and  $pair\_data.y$ . Calculate  $x\_slope\_resid$ , the residuals  
957 between the  $dh\_fit\_dx$  and  $x\_slope\_resid$  for all segments for this reference point,  $seg\_x\_center$   
958 and  $y\_polyfit\_ctr$ .

959           4e. Calculate  $x\_slope\_threshold$ , equal to the maximum of either  $mx\_regression\_tol$  or  
960 three times the RDE of  $x\_slope\_resid$  for valid segments.

961           4f. Mark  $valid\_segs.x\_slope$  with  $|x\_slope\_resid| > x\_slope\_threshold$  as invalid. Re-  
962 establish  $valid\_pairs.x\_slope$  when both  $valid\_segs.x\_slope$  equal 1. Re-establish  
963  $pairs\_valid\_for\_x\_fit$ . Return to step 4d (allow two iterations total).

964           4g. After the second repetition of 4d-f, mark all segments with  $|x\_slope\_resid|$  less than  
965  $x\_slope\_threshold$  with 1 in  $seg\_valid\_xslope$ , 0 otherwise. Define  $valid\_pairs.x\_slope$  as 1 for  
966 pairs that contain two segments with  $valid\_segs.x\_slope=1$ , 0 otherwise.

967           5. Re-establish  $valid\_pairs.all$ . Set equal to 1 if  $valid\_pairs.x\_slope$ ,  $valid\_pairs.y\_slope$ ,  
968 and  $valid\_pairs.data$  are all valid.

969           5a. Identify  $unselected\_cycle\_segs$ , as those  $D6.cycles$  where  $valid\_pairs.all$  are False.

970

971

972 **5.1.3 Adjust the reference-point y location to include the maximum number of**  
 973 **cycles**

974 **Inputs:**

975 *D\_ATL06*: ATL06 structure for the current reference point.

976 *valid\_pairs*: Pairs selected based on parameter values and along- and across-track slopes.

977 **Outputs:**

978 *ref\_surf/y\_atc*: Adjusted fit-point center *y*.

979 *valid\_pairs*: validity masks for pairs, updated to include those identified as valid based on the  
 980 spatial search around *y\_atc\_ctr*.

981 **Parameters:**

982 *L\_search\_XT*: Across-track search length (equal to 110 m)

983 **Algorithm:**

984 1. Define *y0* as the median of the unique integer values of the pair center *y\_atc* for all  
 985 valid pairs. Set a range of *y* values, *y0\_shifts*, as  $\text{round}(y0) \pm 100$  meters in 2-meter increments.

986 2. For each value of *y0\_shifts* (*y0\_shift*), set a counter, *selected\_seg\_cycle\_count*, to the  
 987 number of distinct cycles for which both segments of the pair are contained entirely within the *y*  
 988 interval [*y0\_shift* - *L\_search\_XT*, *y0\_shift* + *L\_search\_XT*]. Add to this, the number of distinct  
 989 cycles represented by unpaired segments contained within that interval, weighted by 0.01. The  
 990 sum is called *score*.

991 3. Search for an optimal *y*-center value (with the most distinct cycles). Set *y\_best* to the  
 992 value of *y0\_shift* that maximizes *score*. If there are multiple *y0\_shift* values with the same,  
 993 maximum *score*, set to the median of the *y0\_shift* values with the maximum *score*.

994 4. Update *valid\_pairs* to include all pairs with *y\_atc* within  $\pm L\_search\_XT$  from  
 995 *y\_atc\_ctr*.

996 **5.1.4 Calculate the reference surface and corrected heights for selected pairs**

997 **Inputs:**

998 *D\_ATL06*: ATL06 structure for the current reference point, containing parameters for each  
 999 segment:

1000 *x\_atc*: along-track coordinate

1001 *y\_atc*: across-track coordinate

1002 *delta\_t*: time for the segment

1003 *pair\_data*: Structure containing information about ATL06 pairs. Must include:

1004 *y\_atc*: Pair-center across-track coordinates

1005 *valid\_pairs*: Pairs selected based on parameter values and along- and across-track slope.

1006 *x\_atc\_ctr*: The reference point along-track x coordinate (equal to *ref\_surf/x\_atc*).

1007 *y\_atc\_ctr*: The reference point along-track x coordinate (equal to *ref\_surf/y\_atc*)

1008 **Outputs:**

1009 *ref\_surf/deg\_x*: Degree of the reference-surface polynomial in the along-track direction

1010 *ref\_surf/deg\_y*: Degree of the reference-surface polynomial in the across-track direction

1011 *ref\_surf/poly\_coeffs*: Polynomial coefficients of the reference-surface fit

1012 *ref\_surf/poly\_coeffs\_sigma*: Formal error in polynomial coefficients of the reference-surface fit

1013 *r\_seg*: Segment residuals from the reference-surface model

1014 */ptx/h\_corr*: Partially filled-in per-cycle corrected height for cycles used in reference surface

1015 */ptx/h\_corr\_sigma*: Partially filled-in per-cycle formal error in corrected height for cycles used in  
 1016 reference surface  
 1017 *ref\_surf\_cycles*: A list of cycles used in defining the reference surface  
 1018 *C\_m\_surf*: Covariance matrix for the reference-polynomial and surface-change model  
 1019 *fit\_columns\_surf*: Mask identifying which components of the combined reference-polynomial  
 1020 and surface-change model were included in the fit.  
 1021 *poly\_exponent\_x*: The x degrees corresponding to the columns of matrix used in fitting the  
 1022 reference surface to the data  
 1023 *poly\_exponent\_y*: The y degrees corresponding to the columns of matrix used in fitting the  
 1024 reference surface to the data  
 1025 *selected\_segments*: A set of flags indicating which segments were selected by the iterative  
 1026 fitting process.  
 1027 Partially filled-n per-cycle ATL11 output variables (see table 4-3) for cycles used in reference  
 1028 surface  
 1029 **Parameters:**  
 1030 *poly\_max\_degree\_AT*: Maximum polynomial degree for the along-track fit, equal to 3.  
 1031 *poly\_max\_degree\_XT*: Maximum polynomial degree for the across-track fit, equal to 2.  
 1032 *max\_fit\_iterations*: Maximum number of iterations for surface fitting, with acceptable residuals,  
 1033 equal to 20.  
 1034 *xy\_scale*: The horizontal scaling value used in polynomial fits, equal to 100 m  
 1035 *t\_scale*: The time scale used in polynomial fits, equal to seconds in 1 year.  
 1036 **Algorithm:**  
 1037 1. Build the cycle design matrix: **G\_zp** is a matrix that has one column for each distinct  
 1038 cycle in *selected\_pairs* and one row for each segment whose pair is in *selected\_pairs*. For each  
 1039 segment, the corresponding row of **G\_zp** is 1 for the column matching the cycle for that segment  
 1040 and zero otherwise.  
 1041 2. Select the polynomial degree.  
 1042 The degree of the x polynomial, *ref\_surf/deg\_x*, is:  
 1043  $\min(\text{poly\_max\_degree\_AT}, \text{maximum}(\text{number of distinct values of } \text{round}((x\_atc - x\_atc\_ctr)/20)$   
 1044  $\text{among the selected segments in any one cycle}) - 1)$ , and the degree of the y polynomial,  
 1045 *ref\_surf/deg\_y*, is :  $\min(\text{poly\_max\_degree\_XT}, \text{number of distinct values of}$   
 1046  $\text{round}((\text{pair\_data.y\_atc} - \text{y\_atc\_ctr})/20)$  among the selected pairs)  
 1047 3. Perform an iterative fit for the reference-surface polynomial.  
 1048 3a. Define *degree\_list\_x* and *degree\_list\_y*: This array defines the x and y degree of the  
 1049 polynomial coefficients in the polynomial surface model. There is one component for each  
 1050 unique degree combination of x degrees between 0 and *ref\_surf/deg\_x* and for y degree between  
 1051 0 and *ref\_surf/deg\_y* such that  $x\_degree + y\_degree \leq \max(\text{ref\_surf/deg\_x}, \text{ref\_surf/deg\_y})$ ,  
 1052 except that there is no  $x\_degree=0$  and  $y\_degree=0$  combination. They are sorted first by the  
 1053 sum of the x and y degrees, then by x degree, then by y degree.  
 1054 3b. Define the polynomial fit matrix. **S\_fit\_poly** has one column for each element of  
 1055 the polynomial degree arrays, with values equal to  $((x\_atc - x\_atc\_ctr)/xy\_scale)^{x\_degree} ((y\_atc -$   
 1056  $y\_atc\_ctr)/xy\_scale)^{y\_degree}$ . There is one row in the matrix for every segment marked as *selected*.  
 1057 3d. Build the surface matrix, **G\_surf**, and the combined surface and cycle-height matrix,  
 1058 **G\_surf\_zp**: The surface matrix is equal to **S\_fit\_poly**. The combined surface and cycle-height  
 1059 matrix, **G\_surf\_zp**, is equal to the horizontal catenation of **G\_surf** and **G\_zp**.

1060           3e. Subset the fitting matrix. Subset **G\_surf\_zp** by row to include only rows  
1061 corresponding to selected segments to produce **G** (on the first iteration, all are *selected*). Next,  
1062 subset **G** by column, first to eliminate all-zero columns, and second to include only columns that  
1063 are linearly independent from one another: calculate the normalized correlation between each  
1064 pair of columns in **G**, and if the correlation is equal to unity, eliminate the column with the  
1065 higher weighted degree ( $poly\_wt\_sum = x\_degree + 1.1*y\_degree$ , with the factor of 1.1  
1066 chosen to avoid ties). Identify the selected columns in the matrix as *fit\_columns*. If more than  
1067 three of the original surface-change columns have been eliminated, set the  
1068 *ref\_surf/complex\_surface\_flag* to *True*, mark all columns corresponding to polynomial  
1069 coefficients of combined x and y degree greater than 1 as *False* in *fit\_columns*.

1070           3f. Check whether the inverse problem is under- or even-determined: If the number of  
1071 *selected\_segments* is less than the number of columns of **G**, eliminate remaining columns of **G** in  
1072 descending order of *poly\_wt\_sum* until the number of columns of **G** is less than the number of  
1073 *selected\_segments*.

1074           3g. Generate the data-covariance matrix, **C\_d**. The data-covariance matrix is a square  
1075 matrix whose diagonal elements are the squares of the *h\_li\_sigma* values for the selected  
1076 segments.

1077           3h. Calculate the polynomial fit. Initialize **m\_surf\_zp**, the reference model, to a vector of  
1078 zero values, with one value for each column of **G\_surf\_zp**. Calculate the generalized inverse  
1079 (equation 7), of **G**, **G\_g**. If the inversion calculation returns an error, or if any row of **G\_g** is all-  
1080 zero (indicating some parameters are not linearly independent), report fit failure and return.  
1081 Otherwise, multiply **G\_g** by the subset of *h\_li* corresponding to the selected segment to give **m**,  
1082 containing values for the parameters selected in *fit\_columns*. Fill in the components of  
1083 **m\_surf\_zp** flagged in *fit\_columns* with the values in **m**.

1084           3i. Calculate model residuals for all segments, *r\_seg*, equal to  $h\_li - G\_surf\_dz * m\_surf\_zp$ .  
1085 The subset of *r\_seg* corresponding to *selected* segments is *r\_fit*.

1086           3j. Calculate the fitting tolerance, *r\_tol*, equal to three times the RDE of the  
1087  $r\_fit/h\_li\_sigma$  for all *selected* segments. Calculate the reduced chi-squared value for these  
1088 residuals, *ref\_surf/misfit\_chi2*, equal to  $r\_fit^T C\_d^{-1} r\_fit$ . Calculate the *P* value for the misfit,  
1089 equal to one minus the CDF of a chi-squared distribution with *m-n* degrees of freedom for  
1090 *ref\_surf/misfit\_chi2*, where *m* is the number of rows in **G**, and *n* is the number of columns.

1091           3k. If the *P* value is less than 0.025 and fewer than *max\_fit\_iterations* have taken place,  
1092 mark all segments for which  $|r\_seg/h\_li\_sigma| < r\_tol$  as *selected*, and return to 3e. Otherwise,  
1093 continue to 3k.

1094           3l. Propagate the errors. Based on the most recent value of **C\_d**, generate a revised data-  
1095 covariance matrix, **C\_dp**, whose diagonals values are the maximum of  $h\_li\_sigma^2$  and  
1096  $RDE(r\_fit)^2$ . Calculate the model covariance matrix, **C\_m** using equation 9. If any of the  
1097 diagonal elements of **C\_m** are larger than  $10^4$ , report a fit failure and return. Fill in elements of  
1098 **m\_surf\_zp** that are marked as valid in *fit\_columns* with the square roots of the corresponding  
1099 diagonal elements of **C\_m**. If any of the errors in the polynomial coefficients are larger than 10,  
1100 set *ref\_surf/fit\_quality*=1.

1101           4. Return a list of cycles used in determining the reference surface in *ref\_surf\_cycles*. These  
1102 cycles have columns in **G** that contain a valid pair, and for which the steps 3e and 3j did not  
1103 eliminate the degree of freedom. For these cycles, partially fill in the values of */ptx/h\_corr* and  
1104 */ptx/h\_corr\_sigma*, from **m** and **m\_sigma**. Similarly, fill in values for  
1105 */ptx/h\_corr\_sigma\_systematic* (Equation 12) and */ptx/delta\_time*, as well as all variables in Table



1106 4-3. Set */ptx/h\_corr*, */ptx/h\_corr\_sigma*, */ptx/h\_corr\_sigma\_systematic* to NaN for those cycles  
 1107 that have uncorrelated error estimates greater than 15 m.  
 1108 Values from Table 4-2 defining the fitted reference surface are also reported including  
 1109 *ref\_surf/poly\_coeffs* and *ref\_surf/poly\_coeffs\_sigma*.  
 1110 Return **C\_m\_surf**, the portion of **C\_m** corresponding to the polynomial components of  
 1111 **C\_m**. Return *selected\_cols\_surf*, the subset of *selected\_cols* corresponding to the surface  
 1112 polynomial.  
 1113 Return the reduced chi-square value for the last iteration, *ref\_surf/misfit\_chi2r*, equal to  
 1114 *ref\_surf/misfit\_chi2/(m-n)*.  
 1115

### 1116 5.1.5 Calculate corrected heights for cycles with no selected pairs.

#### 1117 **Inputs:**

1118 **C\_m\_surf**: Covariance matrix for the reference-surface model.  
 1119 *degree\_list\_x*, *degree\_list\_y*: List of x-, y-, degrees for which the reference-surface calculation  
 1120 attempted an estimate.  
 1121 *selected\_cols\_surf*: Parameters of the reference-surface for which the inversion returned a value.  
 1122 There should be one value for each row/column of **C\_m\_surf**.  
 1123 *x\_atc\_ctr*, *y\_atc\_ctr*: Center point for the surface fit (equal to *ref\_surf/x\_atc*, *ref\_surf/y\_atc*)  
 1124 *selected\_segments*: Boolean array indicating segments selected for the reference-surface  
 1125 calculation  
 1126 *valid\_segs.x\_slope*: Segments identified as valid based on x-slope consistency  
 1127 *valid\_segs.data*: Segments identified as valid based on ATL06 parameter values.  
 1128 *pair\_number*: Pair number for each segment  
 1129 *h\_li*: Land-ice height for each segment  
 1130 *h\_li\_sigma*: Formal error in *h\_li*.  
 1131 */ptx/h\_corr*: Partially filled-in per-cycle corrected height  
 1132 */ptx/h\_corr\_sigma*: Partially filled-in per-cycle corrected height error  
 1133 *ref\_surf/poly\_coeffs*: Polynomial coefficients from 2-d reference-surface fit  
 1134 *ref\_surf\_cycles*: A list of cycles used in defining the reference surface  
 1135 *ref\_surf/N\_slope*, *ref\_surf/E\_slope*: slope components of reference surface  
 1136 *sigma\_geo\_r*: Radial component of the geolocation error for the crossing track  
 1137 *D\_ATL06*: ATL06 data structure  
 1138 Partially filled-in per-cycle ATL11 output variables (see table 4-3)

#### 1139 **Outputs:**

1140 */ptx/h\_corr*: Per-cycle corrected height  
 1141 */ptx/h\_corr\_sigma*: Per-cycle corrected height error  
 1142 *selected\_segments*: A set of arrays listing the selected segments for each cycle.  
 1143 Per-cycle ATL11 output variables (see table 4-3).

#### 1144 **Algorithm:**

1145 1. Identify the segments marked as valid in *valid\_segs.data* and *valid\_segs.x\_slope* that are not  
 1146 members of the cycles in *ref\_surf\_cycles*. Label these as *non\_ref\_segments*.  
 1147 2. Build **G\_other**, a polynomial-fitting matrix for the *non\_ref\_segments*. **G\_other** will include  
 1148 only the polynomial components listed in *degree\_list\_x* and *degree\_list\_y*. Multiply **G\_other** by  
 1149 [*ref\_surf/poly\_coeffs*] to give corrected heights, *z\_kc*.

1150 3. Take the subset of **G\_other** corresponding to the components in *fit\_cols\_surf* to make  
 1151 **G\_other\_surf**. Propagate the polynomial surface errors and surface-height errors for  
 1152 *non\_ref\_segments* based on **G\_other\_surf**, **C\_m\_surf**, and *h\_li\_sigma* using equation  
 1153 11. These errors are *z\_kc\_sigma*.  
 1154 4. Identify the segments in *non\_ref\_segments* for each cycle, and, from among these, select the  
 1155 one with the smallest *z\_kc\_sigma*. If, for this cycle, *z\_kc\_sigma* is less than 15 m, fill in the  
 1156 corresponding values of */ptx/h\_corr* and */ptx/h\_corr\_sigma*. For cycles containing no valid  
 1157 segments, report invalid data as NaN. Similarly, fill in the variables in Table 4-3, with the value  
 1158 from the segment with the smallest *z\_kc\_sigma*.  
 1159

### 1160 **5.1.6 Calculate corrected heights for crossover data points**

#### 1161 **Inputs:**

1162 *C\_m\_surf*: Covariance matrix for the reference surface model.  
 1163 *C\_m\_surf*: Covariance matrix for the reference-surface model.  
 1164 *x\_atc\_ctr*, *y\_atc\_ctr*: Center point for the surface fit, in along-track coordinates  
 1165 *lat\_d*, *lon\_d*: Latitude and longitude for the adjusted datum reference point (from */ptx/latitude*,  
 1166 */ptx/longitude*)  
 1167 *PT*: Pair track for the surface fit  
 1168 *RGT*: RGT for the surface fit  
 1169 *ref\_surf/rgt\_azimuth*: The azimuth of the RGT, relative to local north  
 1170 *lat\_c*, *lon\_c*: Location for crossover data  
 1171 *time\_c*: Time for crossover data  
 1172 *h\_c*: Elevations for crossover data  
 1173 *sigma\_h\_c*: Estimated errors for crossover data  
 1174 *along\_track\_shift\_table*: Estimated geolocation bias lookup table (*delta\_x\_atc*, *delta\_y\_atc* vs.  
 1175 *delta\_time*)  
 1176

#### 1177 **Outputs:**

1178 *ref\_pt*: reference point (for the reference track)  
 1179 *pt*: pair track for the crossing-track points  
 1180 *crossing\_track\_data/rgt*: Reference ground track for the crossing-track point  
 1181 *crossing\_track\_data/delta\_time*: time for the crossing-track point  
 1182 *crossing\_track\_data/h\_corr*: corrected elevation for the crossing-track points  
 1183 *crossing\_track\_data/h\_corr\_sigma*: error in the corrected elevation for the crossing\_track points  
 1184 *crossing\_track\_data/h\_corr\_sigma\_systematic*: Error component in the corrected elevation due  
 1185 to pointing and orbital errors.  
 1186 *crossing\_track\_data/along\_track\_rss*:

#### 1187 **Parameters:**

1188 *L\_search\_XT*: Across-track search distance

#### 1189 **Algorithm (executed independently for the data from each cycle of the mission):**

1190 Steps 1, 2, and 3 are only carried out for Antarctic data. For Arctic data,  
 1191 *along\_track\_shift\_table* is not specified, and the algorithm begins on step  
 1192 1. Calculate *x\_spot* and *y\_spot* using equation 17, assuming that the satellite elevation  
 1193 above the ellipsoid is 511 km

- 1194 2. Interpolate  $\Delta x_{ATC}$  and  $\Delta y_{ATC}$  from *along\_track\_shift\_table* as a function  
 1195 of time.
- 1196 3. Calculate the corrected height using equation 19. Assign the difference between  
 1197 corrected height and uncorrected height to the  $dh_{geoloc}$  variable in the  
 1198 *crossing\_track\_data* structure.
- 1199 4. Project data points into the along-track coordinate system:
- 1200 4a: Calculate along-track and across-track vectors:
- 1201  $x_{hat} = [\cos(\text{ref\_surf}/\text{rgt\_azimuth}), \sin(\text{ref\_surf}/\text{rgt\_azimuth})]$   
 1202  $y_{hat} = [\sin(\text{ref\_surf}/\text{rgt\_azimuth}), -\cos(\text{ref\_surf}/\text{rgt\_azimuth})]$
- 1203 4b. Calculate the  $R_{earth}$ , the WGS84 radius at  $lat_d$ .
- 1204 4c: Project the crossover data points into a local projection centered on the fit center:
- 1205  $N_d = R_{earth} (lat_c - lat_d)$   
 1206  $E_d = R_{earth} \cos(lat_d) (lon_c - lon_d)$
- 1207 4d: Calculate the x and y coordinates for the data points, relative to the fit-center point:
- 1208  $dx_c = \langle x_{hat}, [E_c, N_c] \rangle$   
 1209  $dy_c = \langle y_{hat}, [E_c, N_c] \rangle$
- 1210 Here  $\langle \mathbf{a}, \mathbf{b} \rangle$  is the inner (dot) product of  $\mathbf{a}$  and  $\mathbf{b}$ .
- 1211 5. Calculate the fitting matrix using equation 6.
- 1212 6. Calculate the errors at each point using the fitting matrix and  $C_m$ , using on equation 11.
- 1213 7. Select the minimum-error data point and report the values in Table 4-1.
- 1214 8. Calculate the systematic error in the corrected height:
- 1215  $\text{crossing\_track\_data}/h\_sigma\_sigma\_systematic = (\sigma_{geo\_r^2} + (N_d$   
 1216  $\text{ref\_surf}/n\_slope)^2 + (E_d \text{ref\_surf}/e\_slope)^2)^{1/2}$
- 1217 9. Calculate the along-track RSS for the selected segment. For each selected crossing segment  
 1218 calculate the endpoint heights (equal to the segment center height plus or minus 20 meters times  
 1219 the segment's along-track slope), and calculate the RSS of the differences between these heights  
 1220 and the center heights of the previous and subsequent segments. If this RSS difference is greater  
 1221 than 10 m for any cycle, do not report any parameters for that segment's cycle.

### 1222 5.1.7 Provide error-averaged values for selected ATL06 parameters

#### 1223 **Inputs:**

1224 *ATL06 data structure*: ATL06 data to be averaged

1225 *Selected\_segments*: A set of arrays listing the selected segments for each cycle.

1226 *Parameter\_list*: A list of parameters to be averaged

#### 1227 **Outputs:**

1228 *Parameter\_averages*: One value for each parameter and each cycle

#### 1229 **Algorithm:**

- 1230 1. For each cycle, select the values of  $h_{li\_sigma}$  based on the values within *selected\_segments*.  
 1231 Calculate a set of weights,  $w_i$ , such that the sum of the weights is equal to 1 and each weight is  
 1232 proportional to the inverse square of  $h_{li\_sigma}$ . If only one value is present in  
 1233 *selected\_segments*,  $w_1 = 1$ .
- 1234 2. For each parameter, multiply the weights for each cycle by the parameter values, report the  
 1235 averaged value in *parameter\_averages*.

1236 **5.1.8 Provide miscellaneous ATL06 parameters**

1237 **Inputs:**

1238 *ATL06 data structure*: ATL06 data to be averaged

1239 *Selected\_segments*: A set of arrays listing the selected segments for each cycle.

1240 **Outputs:**

1241 Weighted-averaged parameter values, with one value per cycle, filled in with NaN for cycles  
1242 with no selected segments

1243 *cycle\_stats/h\_robust\_sprd*

1244 *cycle\_stats/h\_li\_rms\_mean*

1245 *cycle\_stats/r\_eff*

1246 *cycle\_stats/tide\_ocean*

1247 *cycle\_stats/dac*

1248 *cycle\_stats/bsnow\_h*

1249 *cycle\_stats/x\_atc*

1250 *cycle\_stats/y\_atc*

1251 *cycle\_stats/sigma\_geo\_h*

1252 *cycle\_stats/sigma\_geo\_at*

1253 *cycle\_stats/sigma\_geo\_xt*

1254 *cycle\_stats/h\_mean*

1255 *ref\_surf/dem\_h*

1256 *ref\_surf/geoid\_h*

1257 Parameter minimum values, with one value per cycle, filled in NaN for cycles with no selected  
1258 segments:

1259 *cycle\_stats/cloud\_flg\_asr*

1260 *cycle\_stats/cloud\_flg\_atm*

1261 *cycle\_stats/bsnow\_conf*

1262 Other parameters:

1263 *cycle\_stats/strong\_spot*: The laser beam number for the strong beam in the pair

1264 **Algorithm:**

1265 1. Select the segments for the cycle indicated in *selected\_segments* from the  
1266 *ATL06\_data\_structure*.

1267 2: Based on *h\_li\_sigma*, calculate the segment weights using equation 14.

1268 3.1 For ATL06 parameters *h\_robust\_sprd*, *h\_li\_rms*, *r\_eff*, *tide\_ocean*, *dac*, *bsnow\_h*, *x\_atc*,  
1269 *y\_atc*, *sigma\_geo\_h*, *sigma\_geo\_at*, *sigma\_geo\_xt*, and *h\_mean* calculate the weighted average  
1270 of the parameter based on the segment weights. The output parameter names are the same as the  
1271 input parameter names, in the *cycle\_stats* group.

1272 3.2 For ATL06 parameters *dem\_h* and *geoid\_h*, by regression between the measurement  
1273 location and the reference point location. The output parameter names are the same as the input  
1274 parameter names, in the *ref\_surf* group.

1275 4. For ATL06 parameters *cloud\_flg\_asr* and *cloud\_flg\_atm* report the best (minimum) value  
1276 from among the selected values. For *bsnow\_conf* report the maximum value from among the  
1277 selected values.

1278 5. For the *cycle\_stats/strong\_spot* attribute, report the laser beam number for the strong beam in  
1279 the pair.

1280

1281 **5.1.9 Characterize the reference surface**

1282 **Inputs:**

1283 *poly\_coeffs*: Coefficients of the surface polynomial

1284 *poly\_coeff\_sigma*: Error estimates for the surface polynomial

1285 *degree\_list\_x*, *degree\_list\_y*: exponents of the reference-surface polynomial for which the  
1286 reference-surface fit returned a coefficient

1287 *rgt\_azimuth*: the azimuth of the reference ground track

1288 **Parameters:**

1289 *poly\_max\_degree\_AT*, *poly\_max\_degree\_XT*: Maximum polynomial degree allowed in x and y.

1290 **Outputs:**

1291 *ref\_surf/n\_slope*: the north component of the reference-surface slope

1292 *ref\_surf/e\_slope*: the east component of the reference-surface slope

1293 *ref\_surf/at\_slope*: the along-track component of the reference-surface slope

1294 *ref\_surf/xt\_slope*: the across-track component of the reference-surface slope

1295 *ref\_surf/rms\_slope\_fit*: the rms slope of the reference surface

1296 *ref\_surf/poly\_ref\_surf*: the polynomial reference surface coefficients

1297 *ref\_surf/poly\_ref\_surf\_sigma*: error estimates for *ref\_surf/poly\_ref\_surf*

1298 **Procedure:**

1299 1. Calculate the coordinates of a grid of northing and easting offsets around the reference points,  
1300 each between -50 m and 50 m in 10-meter increments: *dN*, *dE*

1301 2. Translate the coordinates into along and across-track coordinates:

1302  $dx = \cos(rgt\_azimuth) * dN + \sin(rgt\_azimuth) * dE$

1303  $dy = \sin(rgt\_azimuth) * dN - \cos(rgt\_azimuth) * dE$

1304 3. Calculate the polynomial surface elevations for the grid points by evaluating the polynomial  
1305 surface at *dx* and *dy*: *z\_poly*

1306 4. Fit a plane to *z\_poly* as a function of *dN* and *dE*. The North coefficient of the plane is  
1307 *ref\_surf/n\_slope*, the east component is *ref\_surf/e\_slope*, the RMS misfit of the plane is

1308 *ref\_surf/rms\_slope\_fit*. If either component of the slope has a magnitude larger than 0.2, add 2 to  
1309 *ref\_surf/fit\_quality*.

1310 5. Fit a plane to *z\_poly* as a function of *dx* and *dy*. The along-track coefficient of the plane is  
1311 *ref\_surf/at\_slope*, the across-track component is *ref\_surf/xt\_slope*.

1312 6. Generate the polynomial exponents for the output columns. The list of components for  
1313 the output variables has one component for each unique degree combination of *x* degrees  
1314 between 0 and *ref\_surf/deg\_x* and for *y* degree between 0 and *ref\_surf/deg\_y* such that *x\_degree*  
1315 + *y\_degree*  $\leq \max(\text{poly\_max\_degree\_XT}, \text{poly\_max\_degree\_AT})$ , except that there is no  
1316 *x\_degree=0* and *y\_degree=0* combination. They are sorted first by the sum of the *x* and *y*  
1317 degrees, then by *x* degree, then by *y* degree.

1318 Match the polynomial degrees for this reference point's coefficients to these degrees, and write  
1319 each value of *poly\_ref\_surf* and *poly\_ref\_surf\_sigma* into the appropriate position of the output  
1320 array, filling missing values with *invalid*.

1321

1322 **6.0 APPENDIX A: GLOSSARY**

1323 This appendix defines terms that are used in ATLAS ATBDs, as derived from a document  
 1324 circulated to the SDT, written by Tom Neumann. Some naming conventions are borrowed from  
 1325 **Spots, Channels and Redundancy Assignments** (ICESat-2-ATSYS-TN-0910) by P. Luers.  
 1326 Some conventions are different than those used by the ATLAS team for the purposes of making  
 1327 the data processing and interpretation simpler.

1328  
 1329 **Spots.** The ATLAS instrument creates six spots on the ground, three that are weak and three that  
 1330 are strong, where strong is defined as approximately four times brighter than weak. These  
 1331 designations apply to both the laser-illuminated spots and the instrument fields of view. The  
 1332 spots are numbered as shown in Figure 1. At times, the weak spots are leading (when the  
 1333 direction of travel is in the ATLAS +x direction) and at times the strong spots are leading.  
 1334 However, the spot number does not change based on the orientation of ATLAS. The spots are  
 1335 always numbered with 1L on the far left and 3R on the far right of the pattern. Not: beams,  
 1336 footprints.

1337  
 1338 **Laser pulse (pulse for short).** Individual pulses of light emitted from the ATLAS laser are  
 1339 called laser pulses. As the pulse passes through the ATLAS transmit optics, this single pulse is  
 1340 split into 6 individual transmit pulses by the diffractive optical element. The 6 pulses travel to  
 1341 the earth's surface (assuming ATLAS is pointed to the earth's surface). Some attributes of a laser  
 1342 pulse are the wavelength, pulse shape and duration. Not: transmit pulse, laser shot, laser fire.

1343  
 1344 **Laser Beam.** The sequential laser pulses emitted from the ATLAS instrument that illuminate  
 1345 spots on the earth's surface are called laser beams. ATLAS generates 6 laser beams. The laser  
 1346 beam numbering convention follows the ATLAS instrument convention with strong beams  
 1347 numbered 1, 3, and 5 and weak beams numbered 2, 4, and 6 as shown in the figures. Not:  
 1348 beamlet.

1349  
 1350 **Transmit Pulse.** Individual pulses of light emitted from the ICESat-2 observatory are called  
 1351 transmit pulses. The ATLAS instrument generates 6 transmit pulses of light from a single laser  
 1352 pulse. The transmit pulses generate 6 spots where the laser light illuminates the surface of the  
 1353 earth. Some attributes of a given transmit pulse are the wavelength, the shape, and the energy.  
 1354 Some attributes of the 6 transmit pulses may be different. Not: laser fire, shot, laser shot, laser  
 1355 pulse.

1356  
 1357 **Reflected Pulse.** Individual transmit pulses reflected off the surface of the earth and viewed by  
 1358 the ATLAS telescope are called reflected pulses. For a given transmit pulse, there may or may  
 1359 not be a reflected pulse. Not: received pulse, returned pulse.

1360  
 1361 **Photon Event.** Some of the energy in a reflected pulse passes through the ATLAS receiver  
 1362 optics and electronics. ATLAS detects and time tags some fraction of the photons that make up  
 1363 the reflected pulse, as well as background photons due to sunlight or instrument noise. Any  
 1364 photon that is time tagged by the ATLAS instrument is called a photon event, regardless of  
 1365 source. Not: received photon, detected photon.

1366

1367 **Reference Ground Track (RGT).** The reference ground track (RGT) is the track on the earth at  
1368 which a specified unit vector within the observatory is pointed. Under nominal operating  
1369 conditions, there will be no data collected along the RGT, as the RGT is spanned by GT2L and  
1370 GT2R (which are not shown in the figures, but are similar to the GTs that are shown). During  
1371 spacecraft slews or off pointing, it is possible that ground tracks may intersect the RGT. The  
1372 precise unit vector has not yet been defined. The ICESat-2 mission has 1387 RGTs, numbered  
1373 from 0001xx to 1387xx. The last two digits refer to the cycle number. Not: ground tracks, paths,  
1374 sub-satellite track.

1375  
1376 **Cycle Number.** Over 91 days, each of the 1387 RGTs will be targeted in the Polar Regions  
1377 once. In subsequent 91-day periods, these RGTs will be targeted again. The cycle number  
1378 tracks the number of 91-day periods that have elapsed since the ICESat-2 observatory entered the  
1379 science orbit. The first 91-day cycle is numbered 01; the second 91-day cycle is 02, and so on.  
1380 At the end of the first 3 years of operations, we expect the cycle number to be 12. The cycle  
1381 number will be carried in the mid-latitudes, though the same RGTs will (in general) not be  
1382 targeted more than once.

1383  
1384 **Sub-satellite Track (SST).** The sub-satellite track (SST) is the time-ordered series of latitude  
1385 and longitude points at the geodetic nadir of the ICESat-2 observatory. In order to protect the  
1386 ATLAS detectors from damage due to specular returns, and the natural variation of the position  
1387 of the observatory with respect to the RGT throughout the orbit, the SST is generally not the  
1388 same as the RGT. Not: reference ground track, ground track.

1389  
1390 **Ground Tracks (GT).** As ICESat-2 orbits the earths, sequential transmit pulses illuminate six  
1391 ground tracks on the surface of the earth. The track width is approximately 10m wide. Each  
1392 ground track is numbered, according to the laser spot number that generates a given ground  
1393 track. Ground tracks are therefore always numbered with 1L on the far left of the spot pattern  
1394 and 3R on the far right of the spot pattern. Not: tracks, paths, reference ground tracks, footpaths.

1395  
1396 **Reference Pair Track (RPT).** The reference pair track is the imaginary line halfway between  
1397 the planned locations of the strong and weak ground tracks that make up a pair. There are three  
1398 RPTs: RPT1 is spanned by GT1L and GT1R, RPT2 is spanned by GT2L and GT2R (and may be  
1399 coincident with the RGT at times), and RPT3 is spanned by GT3L and GT3R. Note that this is  
1400 the planned location of the midway point between GTs. We will not know this location very  
1401 precisely prior to launch. Not: tracks, paths, reference ground tracks, footpaths, pair tracks.

1402  
1403 **Pair Track (PT).** The pair track is the imaginary line half way between the actual locations of  
1404 the strong and weak ground tracks that make up a pair. There are three PTs: PT1 is spanned by  
1405 GT1L and GT1R, PT2 is spanned by GT2L and GT2R (and may be coincident with the RGT at  
1406 times), and PT3 is spanned by GT3L and GT3R. Note that this is the actual location of the  
1407 midway point between GTs, and will be defined by the actual location of the GTs. Not: tracks,  
1408 paths, reference ground tracks, footpaths, reference pair tracks.

1409  
1410 **Pairs.** When considered together, individual strong and weak ground tracks form a pair. For  
1411 example, GT2L and GT2R form the central pair of the array. The pairs are numbered 1 through



1412 3: Pair 1 is comprised of GT1L and GT1R, pair 2 is comprised of GT2L and GT2R, and pair 3 is  
1413 comprised of GT3L and 3R.

1414

1415 **Along-track.** The direction of travel of the ICESat-2 observatory in the orbit frame is defined as  
1416 the along-track coordinate, and is denoted as the +x direction. The positive x direction is  
1417 therefore along the Earth-Centered Earth-Fixed velocity vector of the observatory. Each pair has  
1418 a unique coordinate system, with the +x direction aligned with the Reference Pair Tracks.

1419

1420 **Across-track.** The across-track coordinate is y and is positive to the left, with the origins at the  
1421 Reference Pair Tracks.

1422

1423 **Segment.** An along-track span (or aggregation) of PE data from a single ground track or other  
1424 defined track is called a segment. A segment can be measured as a time duration (e.g. from the  
1425 time of the first PE to the time of the last PE), as a distance (e.g. the distance between the  
1426 location of the first and last PEs), or as an accumulation of a desired number of photons.  
1427 Segments can be as short or as long as desired.

1428

1429 **Signal Photon.** Any photon event that an algorithm determines to be part of the reflected pulse.

1430

1431 **Background Photon.** Any photon event that is not classified as a signal photon is classified as a  
1432 background photon. Background photons could be due to noise in the ATLAS instrument (e.g.  
1433 stray light, or detector dark counts), sunlight, or mis-classified signal photons. Not: noise  
1434 photon.

1435

1436 **h<sub>\*\*</sub>.** Signal photons will be used by higher-level products to determine height above the  
1437 WGS-84 reference ellipsoid, using a semi-major axis (equatorial radius) of 6378137m and a  
1438 flattening of 1/298.257223563. This can be abbreviated as ‘ellipsoidal height’ or ‘height above  
1439 ellipsoid’. These heights are denoted by h; the subscript \*\* will refer to the specific algorithm  
1440 used to determine that elevation (e.g. is = ice sheet algorithm, si = sea ice algorithm, etc...). Not:  
1441 elevation.

1442

1443 **Photon Cloud.** The collection of all telemetered photon time tags in a given segment is the (or  
1444 a) photon cloud. Not: point cloud.

1445

1446 **Background Count Rate.** The number of background photons in a given time span is the  
1447 background count rate. Therefore a value of the background count rate requires a segment of PEs  
1448 and an algorithm to distinguish signal and background photons. Not: Noise rate, background  
1449 rate.

1450

1451 **Noise Count Rate.** The rate at which the ATLAS instrument receives photons in the absence of  
1452 any light entering the ATLAS telescope or receiver optics. The noise count rate includes PEs  
1453 due to detector dark counts or stray light from within the instrument. Not: noise rate,  
1454 background rate, and background count rate.

1455

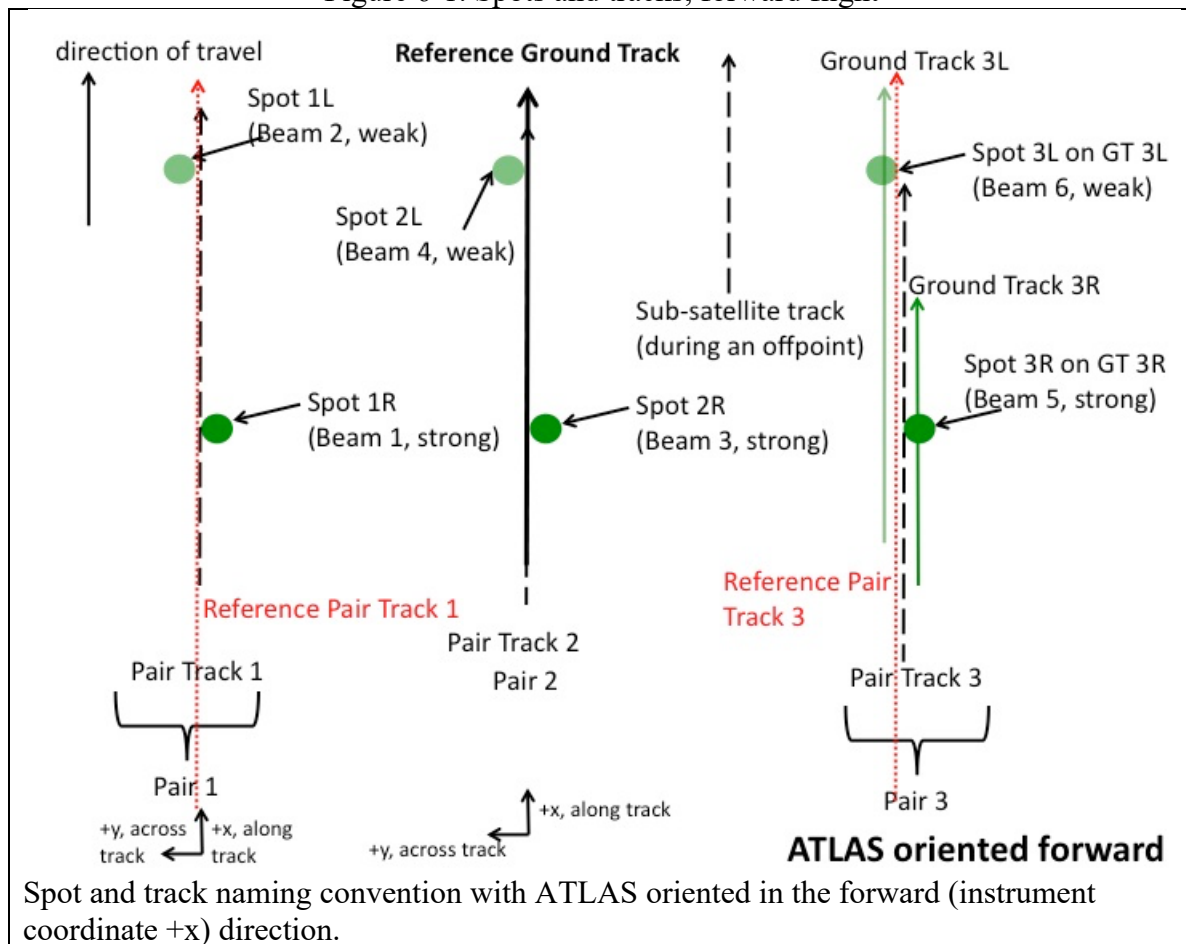
1456 **Telemetry band.** The subset of PEs selected by the science algorithm on board ATLAS to be  
1457 telemetered to the ground is called the telemetry band. The width of the telemetry band is a

1458 function of the signal to noise ratio of the data (calculated by the science algorithm onboard  
 1459 ATLAS), the location on the earth (e.g. ocean, land, sea ice, etc...), and the roughness of the  
 1460 terrain, among other parameters. The widths of telemetry bands are adjustable on-orbit. The  
 1461 telemetry bandwidth is described in Section 7 or the ATLAS Flight Science Receiver Algorithms  
 1462 document. The total volume of telemetered photon events must meet the data volume constraint  
 1463 (currently 577 GBits/day).

1464  
 1465 **Window, Window Width, Window Duration.** A subset of the telemetry band of PEs is called a  
 1466 window. If the vertical extent of a window is defined in terms of distance, the window is said to  
 1467 have a width. If the vertical extent of a window is defined in terms of time, the window is said to  
 1468 have a duration. The window width is always less than or equal to the telemetry band.

1469  
 1470  
 1471  
 1472  
 1473

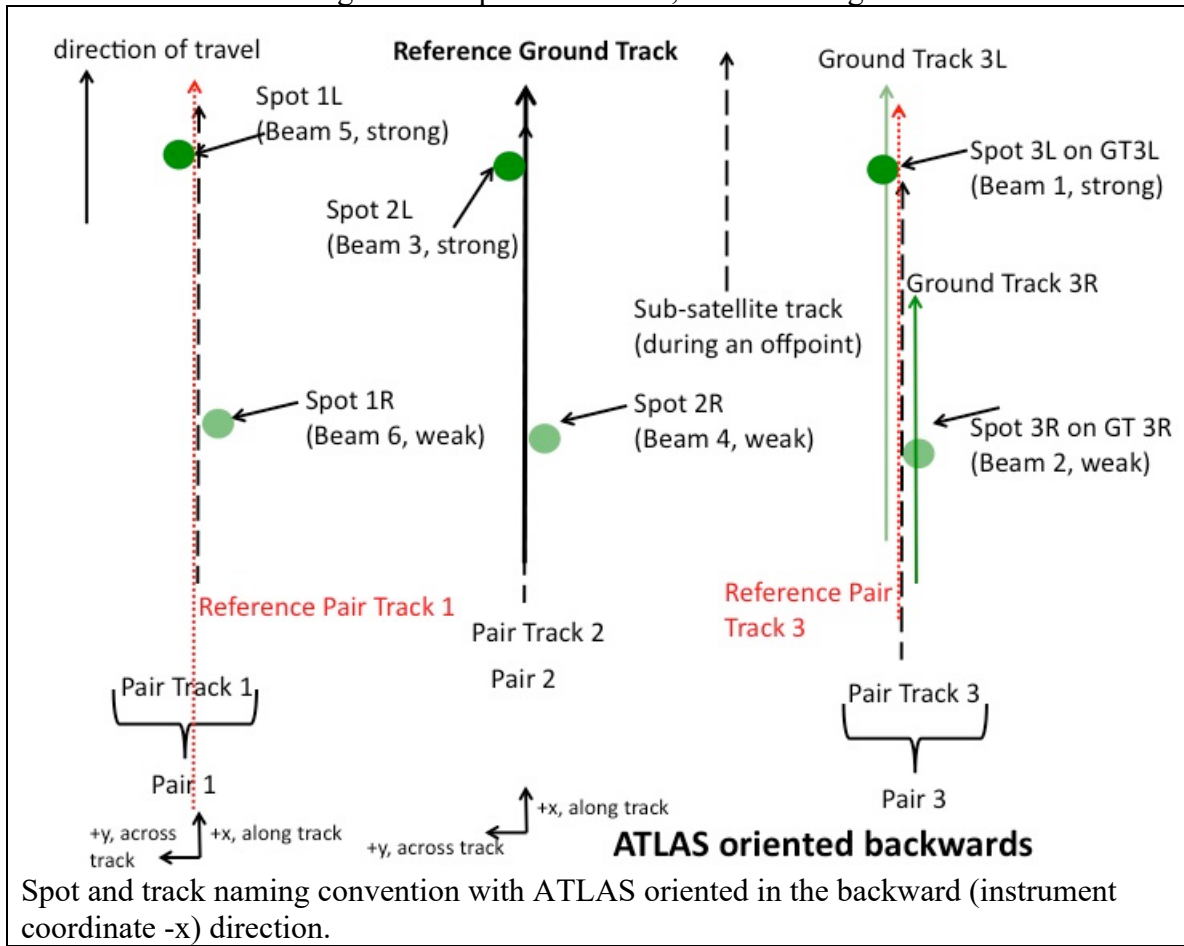
Figure 6-1. Spots and tracks, forward flight



1474  
 1475  
 1476

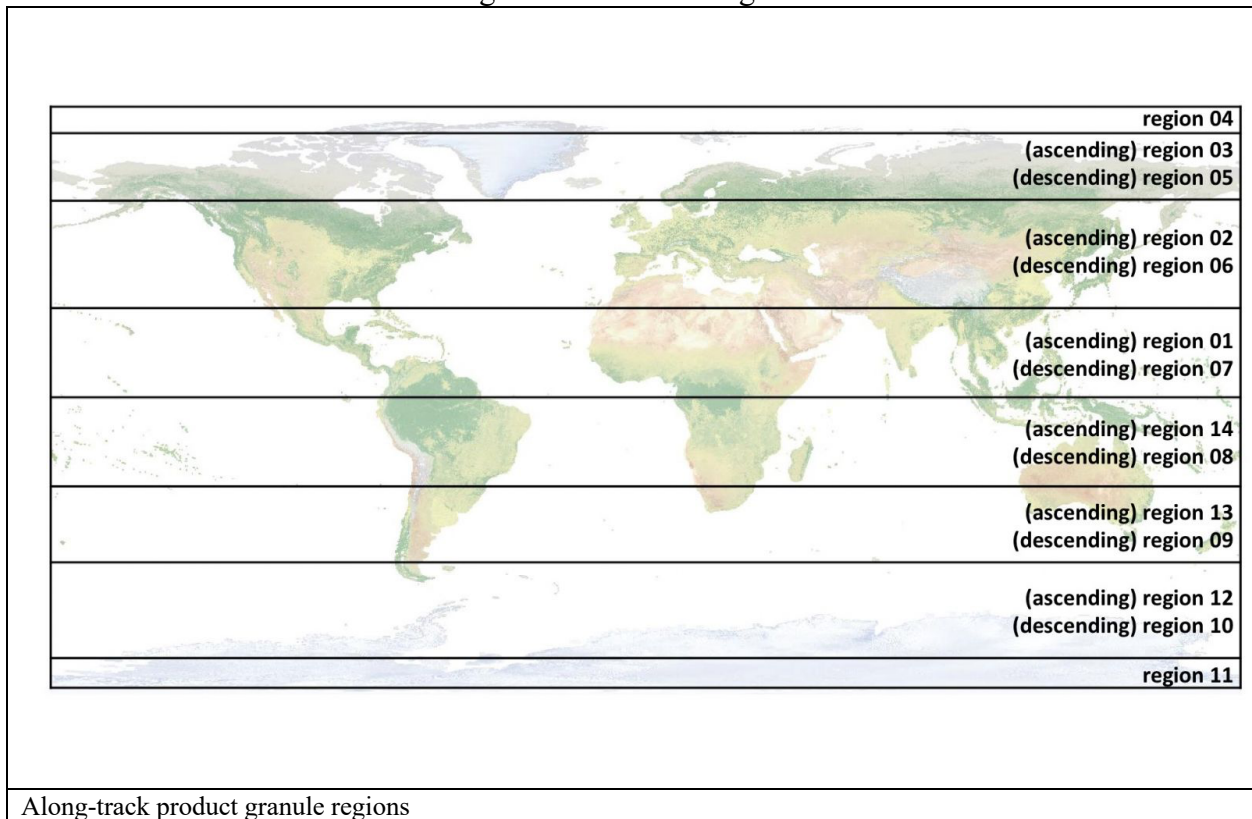
1477  
1478

Figure 6-2. Spots and tracks, backward flight



1479  
1480

Figure 6-3. Granule regions



1481 **7.0 BROWSE PRODUCTS**

1482 For each ATL11 data file, there will be eight figures written to an associated browse file. Two of  
 1483 these figures are required and are located in the default group; default1 and default2. The browse  
 1484 filename has the same pattern as the data filename, namely,  
 1485 ATL11\_tttss\_c1c2\_rr\_vVVV\_BRW.h5, where tttt is the reference ground track, ss is the orbital  
 1486 segment, c1 is the first cycle of data in the file, c2 is the last cycle of data in the file, rr is the  
 1487 release and VVV is the version. Optionally, the figures can also be written to a pdf file.

1488  
 1489 Below is a discussion of the how the figures are made, with examples from the data file  
 1490 ATL11\_009403\_0307\_02\_vU07.h5. Note that the figure numbering in this section is distinct  
 1491 from that in the rest of the document; the figures shown here are labeled as they are in each  
 1492 browse-product file.

1493  
 1494  
 1495

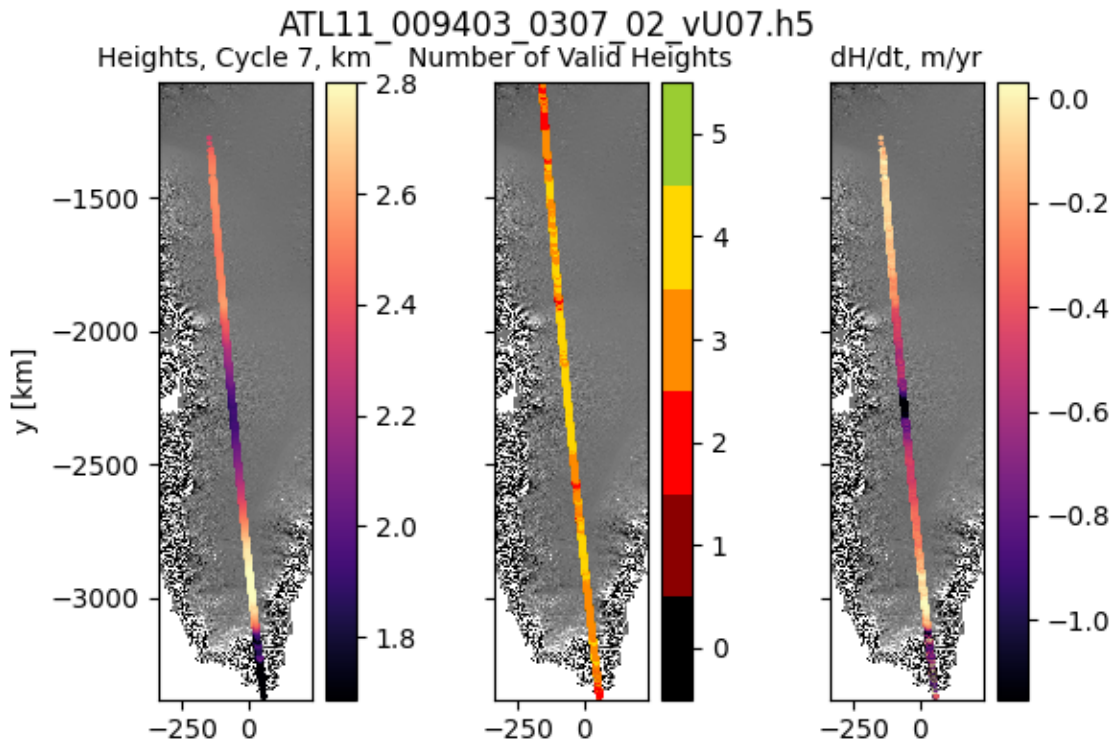


Figure 1. Height data, in km, from cycle 7 (1st panel). Number of cycles with valid height data (2nd panel). Change in height over time, in meters/year, cycle 7 from cycle 3 (3rd panel). All overlaid on gradient of DEM. x, y in km. Maps are plotted in a polar-stereographic projection with a central longitude of 45W and a standard latitude of 70N.

1496  
 1497

1498 The background for the three panels in Figure 1 is the gradient DEM in gray scale. It is shown in  
 1499 a polar-stereographic projection with a central longitude of 45W (0E) and a standard latitude of  
 1500 70N (71S), for the Northern (Southern) Hemisphere. The map is bounded by the extent of height  
 1501 data plus a buffer. ATL11 heights (/ptx/h\_corr) from all pairs of the latest cycle with valid data,

1502 here cycle 7, are plotted in the first panel. The “magma” color map indicates the heights in km.  
 1503 The limits on the color bar are set with the python scipy.stat.scoreatpercentile method at 5% and  
 1504 95%. In the second panel are plotted the number of valid heights summed over all cycles at each  
 1505 location. The color bar extends to the total number of cycles in the data file. The change in height  
 1506 over time,  $dH/dt$ , is plotted in the third panel, in meters/year.  $dHdt$  is the change in height of the  
 1507 last cycle with valid data from the first cycle with valid data ( $/ptx/h\_corr$ ) divided by the  
 1508 associated times ( $/ptx/delta\_time$ ). Text of ‘No Data’ is printed in the panel if there is only one  
 1509 cycle with valid data, or if the first and last cycles with valid data have no common reference  
 1510 point numbers ( $/ptx/ref\_pt$ ). All plots are in x,y coordinates, in km. This figure is called  
 1511 default/default1 in the BRW.h5 file.  
 1512

ATL11\_009403\_0307\_02\_vU07.h5

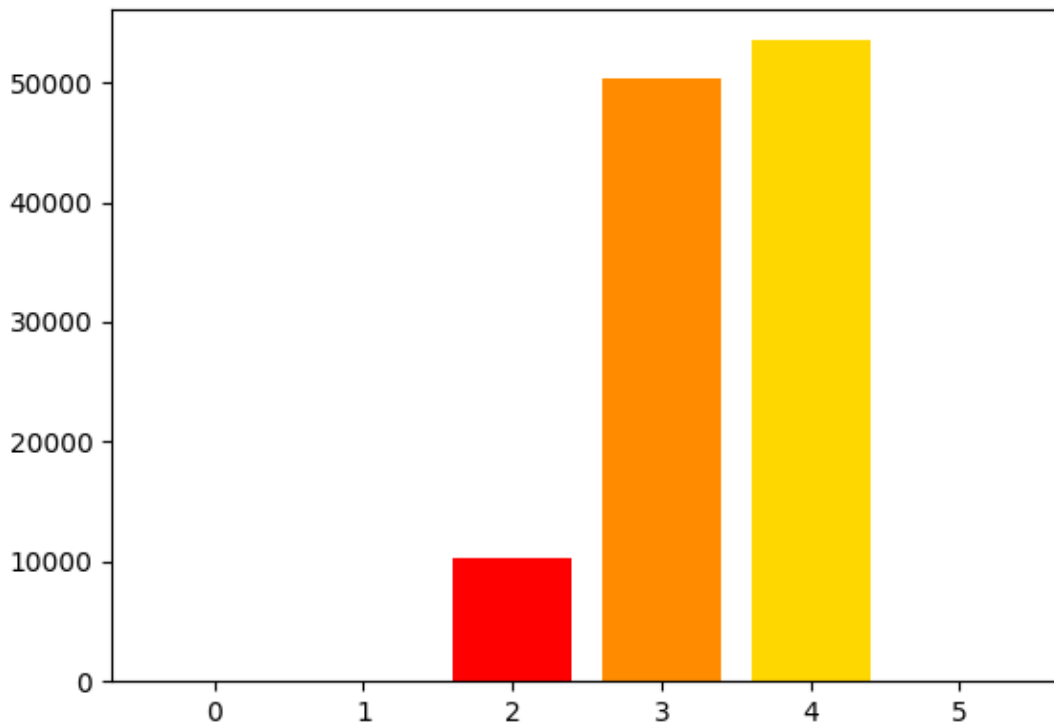


Figure 2. Histogram of number of cycles with valid height measurements, all beam pairs.

1513  
 1514  
 1515 A histogram of the number of valid height measurements ( $/ptx/h\_corr$ ) is in Figure 2. Valid  
 1516 height data are summed across all cycles, for each reference point number ( $/ptx/ref\_pt$ ). The  
 1517 color scale is from zero to the total number of cycles in the data file and matches those in Figure  
 1518 1, 2<sup>nd</sup> panel. This figure is called validrepeats\_hist in the BRW.h5 file.  
 1519

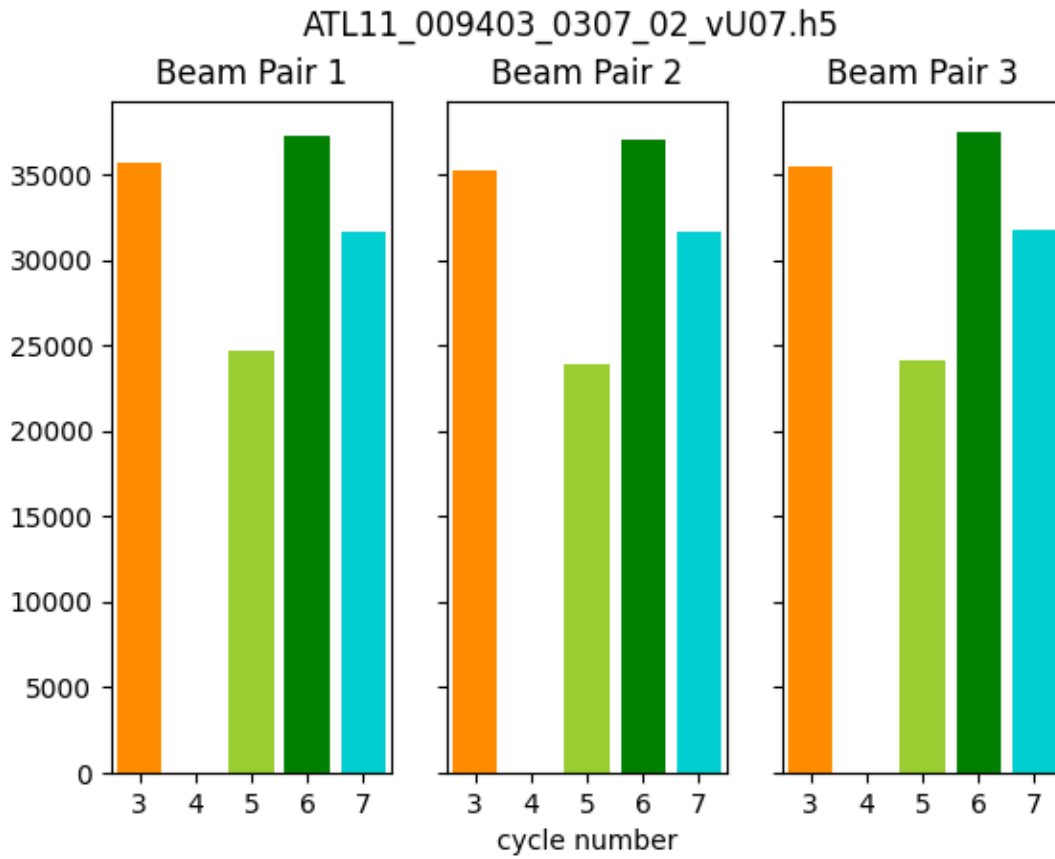


Figure 3. Number of valid height measurements from each beam pair.

1520  
1521  
1522  
1523  
1524  
1525

Histograms in Figure 3 show the number of valid heights (/ptx/h\_corr) for each cycle, separated by beam pair. The cycle numbers are color coded. This figure is called default/default2 in the BRW.h5 file.

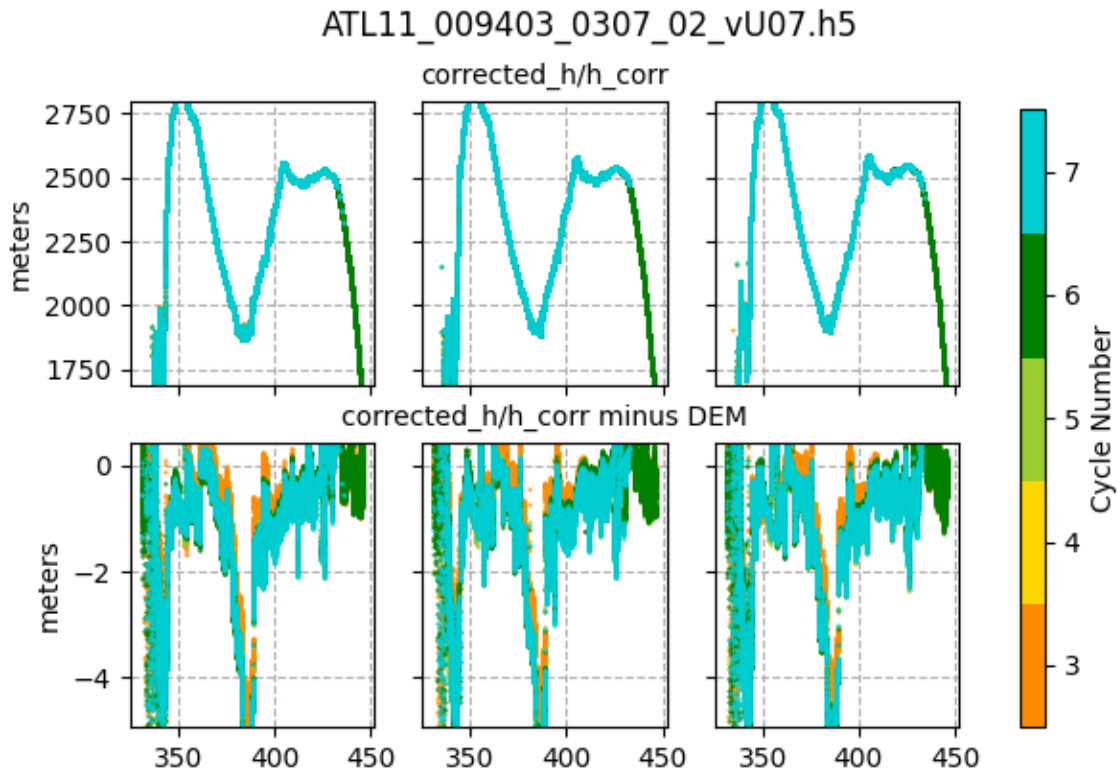


Figure 4. Top row: Heights, in meters, plotted for each beam pair: 1 (left), 2 (center), 3 (right). Bottom row: Heights minus DEM, in meters. Y-axis limits are scores at 5% and 95%. Color coded by cycle number. Plotted against reference point number/1000.

1526  
1527  
1528  
1529  
1530  
1531  
1532  
1533  
1534  
1535  
1536  
1537

There are six panels in Figure 4, with two rows and three columns. In the top row are plotted the height measurements (`/ptx/h_corr`) for each beam pair, one pair per panel. In the bottom row are plotted the same height measurements minus the collocated DEM (`ref_surf/dem_h`) values, one pair per panel. The plots are color coded by cycle number, as in Figure 3. The heights are plotted versus reference point number (`/ptx/ref_pt`) divided by 1000 for a cleaner plot. The y-axis is in meters for both rows. The y-axis limits for the top and bottom rows are set separately, using the `python scipy.stats.scoreatpercentile` method with limits of 5% and 95% for heights and height differences, respectively. Text of 'No Data' is printed in a panel if there are no valid height data for that pair. This figure is called `h_corr_h_corr-DEM` in the `BRW.h5` file.



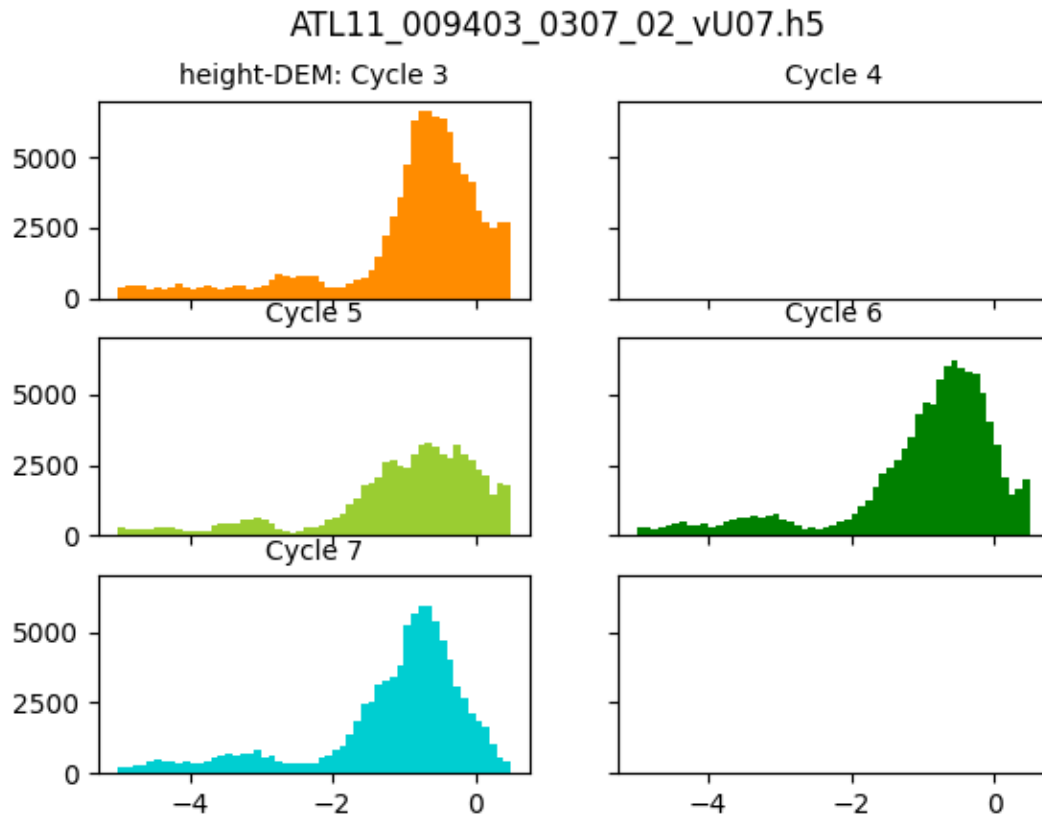


Figure 5. Histograms of heights minus DEM heights, in meters. One histogram per cycle, all beam pairs. X-axis limits are the scores at 5% and 95%.

1538  
 1539  
 1540  
 1541  
 1542  
 1543  
 1544  
 1545  
 1546

Figure 5 is associated with Figure 4. It is a multi-paneled figure, with the number of panels dependent on the number of cycles in the data file. Each panel is a histogram of the heights (/ptx/h\_corr) minus collocated DEM heights (ref\_surf/dem\_h) color coded by cycle, the same as in Figures 3 and 4. The limits on the histograms are set using the python scipy.stats.scoreatpercentile method with limits of 5 and 95% for all cycles of data, the same values used in Figure 4 bottom row. This figure is called h\_corr-DEM\_hist in the BRW.h5 file.

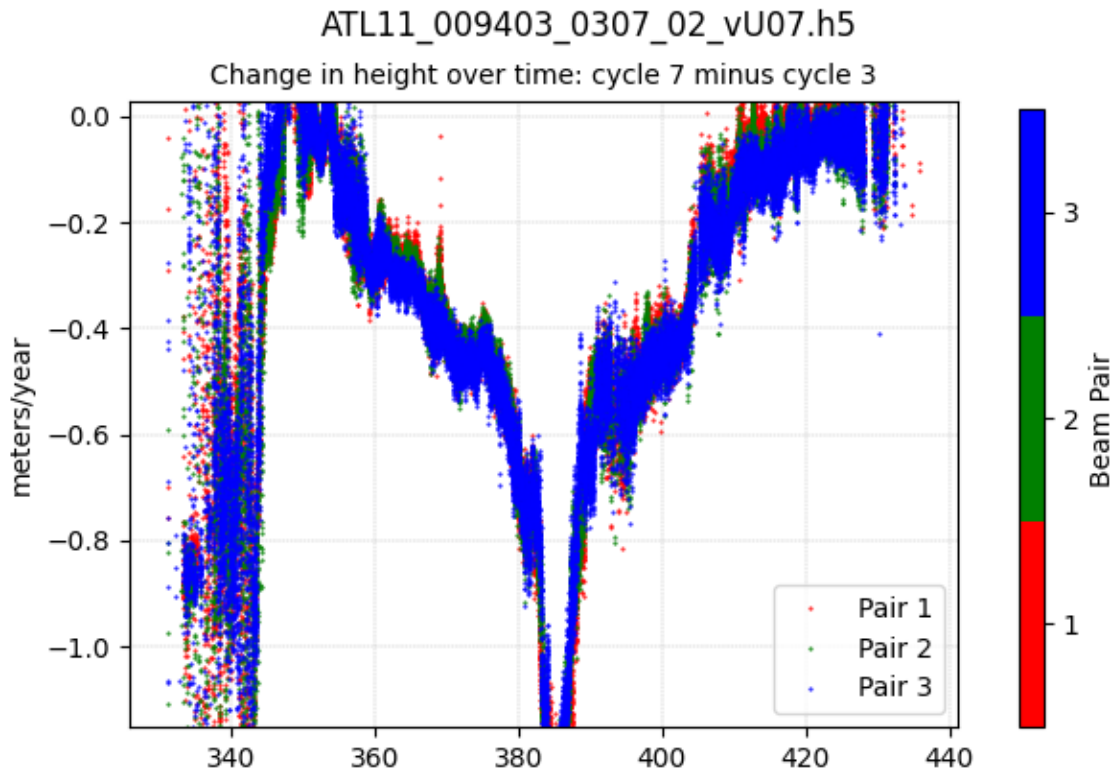


Figure 6. Change in height over time,  $dH/dt$ , in meters/year.  $dH/dt$  is cycle 7 from cycle 3. Color coded by beam pair: 1 (red), 2 (green), 3 (blue). Y-axis limits are scores at 5% and 95%. Plotted against reference point number/1000.

1547  
1548  
1549  
1550  
1551  
1552  
1553  
1554  
1555  
1556  
1557  
1558

The changes in height with time,  $dH/dt$ , in meters/year are plotted in Figure 6. The calculation differences the first and last cycles with valid height data ( $/ptx/h\_corr$ ) divided by the associated time differences ( $/ptx/delta\_time$ ). The change in heights for pair 1 are in red, for pair 2 are in green and for pair 3 are in blue. The y-axis limits are set using the python `scipy.stats.scoreatpercentile` method with limits of 5% and 95%. The x-axis is reference point number ( $/ptx/ref\_pt$ ) divided by 1000 for a cleaner plot. Text of 'No Data' is printed in the panel if there is only one cycle with valid data, or if the first and last cycles with valid data have no common reference point numbers. This figure is called `dHdt` in the `BRW.h5` file.

1559

**Glossary/Acronyms**

ASAS	ATLAS Science Algorithm Software
ATBD	Algorithm Theoretical Basis Document
ATLAS	ATLAS Advance Topographic Laser Altimeter System
CDF	Cumulative Distribution Function
DEM	Digital Elevation Model
GSFC	Goddard Space Flight Center
GTs	Ground Tracks
ICESat-2	Ice, Cloud, and Land Elevation Satellite-2
IKR	I Know, Right?
MABEL	Multiple altimeter Beam Experimental Lidar
MIS	Management Information System
NASA	National Aeronautics and Space Administration
PE	Photon Event
POD	Precision Orbit Determination
PPD	Precision Pointing Determination
PRD	Precise Range Determination
PSO	ICESat-2 Project Science Office
PTs	Pair Tracks
RDE	Robust Dispersion Estimate
RGT	Reference Ground Track
RMS	Root Mean Square
RPTs	Reference Pair Tracks
RT	Real Time
SCoRe	Signature Controlled Request
SIPS	ICESat-2 Science Investigator-led Processing System
TLDR	Too Long, Didn't Read
TBD	To Be Determined

1560

**References**

1561 Brunt, K.M., H.A. Fricker and L. Padman 2011. Analysis of ice plains of the Filchner-Ronne Ice  
1562 Shelf, Antarctica, using ICESat laser altimetry. *Journal of Glaciology*, **57**(205): 965-975.

1563 Fricker, H.A., T. Scambos, R. Bindschadler and L. Padman 2007. An active subglacial water  
1564 system in West Antarctica mapped from space. *Science*, **315**(5818): 1544-1548.

1565 Schenk, T. and B. Csatho 2012. A New Methodology for Detecting Ice Sheet Surface Elevation  
1566 Changes From Laser Altimetry Data. *Ieee Transactions on Geoscience and Remote Sensing*,  
1567 **50**(9): 3302-3316.

1568 Smith, B., H.A. Fricker, N. Holschuh, A.S. Gardner, S. Adusumilli, K.M. Brunt, B. Csatho, K.  
1569 Harbeck, A. Huth, T. Neumann, J. Nilsson and M.R. Siegfried 2019a. Land ice height-retrieval  
1570 algorithm for NASA's ICESat-2 photon-counting laser altimeter. *Remote Sensing of*  
1571 *Environment*: 111352.

1572 Smith, B.E., H.A. Fricker, I.R. Joughin and S. Tulaczyk 2009. An inventory of active subglacial  
1573 lakes in Antarctica detected by ICESat (2003-2008). *Journal of Glaciology*, **55**(192): 573-595.

1574 Smith, B.E., D. Hancock, K. Harbeck, L. Roberts, T. Neumann, K. Brunt, H. Fricker, A.  
1575 Gardner, M. Siegfried, S. Adusumilli, B. Csatho, N. Holschuh, J. Nilsson and F. Paolo 2019b.  
1576 Algorithm Theoretical Basis Document for Land-Ice Along-track Product (ATL06). Goddard  
1577 Space Flight Center.

1578